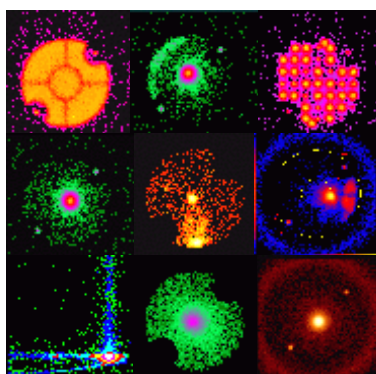


A guided tour to the MECS and to its response matrix



Compiled by L.Chiappetti - IFCTR

online HTML version kept up-to-date at

<http://sax.iasf-milano.inaf.it/Sax/Mecs>

Original idea : February 1997

Public release : October 1998

PostScript snapshot obtained on 02-Nov-2010 16:39

Table of Content

- * [Cover page](#) (only for hardcopy)
 - * [Authors](#) (and the [MECS team](#))
 - * [Table of Content](#) (here)
 - * ftp access to [MECS calibration files](#) (inclusive of update info)
1. [Introduction](#)
 1. [MECS interactive map](#)
 2. [The response matrix : introduction](#)
 1. [Calibration data contributing to the redistribution matrix](#)
 2. [Calibration data contributing to the overall effective area](#)
 3. [Calibration data used in event linearization](#)
 4. [Other calibration data](#)
 5. [MECS background](#)
 2. [The MECS components](#)
 1. [Mirror Unit](#)
 1. [The mirrors](#)
 2. [The spider](#)
 3. [The Plasma suppression grid](#)
 2. [Detector Unit](#)
 1. [The ion shield and UV filter](#)
 2. [The gas cell](#)
 1. [The calibration sources](#)
 2. [The Be window](#)
 3. [The drift region](#)
 4. [The scintillation region](#)

3. [The Photo Multiplier Tube](#)
3. [Electronics Unit](#)
 1. [Front End Electronics](#)
 2. [Event Processor](#)
 3. [Communication Processor](#)
3. [Principles of operation of the ME-GSPC](#)
4. [The MECS calibration parameters](#)
 1. [Mirror effective area](#)
 1. [On-axis area](#)
 2. [Vignetting correction](#)
 3. [Infinity correction](#)
 4. [Focal length](#)
 5. [Misalignments](#)
 2. [Plasma suppression grid transmission](#)
 3. [Filter transmission](#)
 4. [Calibration source parameters](#)
 5. [Beryllium window transmission](#)
 6. [Detector quantum efficiency](#)
 1. [Drift region](#)
 2. [Scintillation region](#)
 7. [Detector resolution](#)
 1. [Gaussian component](#)
 2. [Low energy tail](#)
 8. [Escape fractions](#)
 9. [Linearization coefficients](#)
 10. [MECS gain](#)
 1. [Gain coefficients](#)
 2. [Positional dependency](#)
 3. [Time \(Temperature\) dependency](#)
 4. [Absolute reference](#)
 5. [The channel boundaries](#)
 11. [The Point Spread Function](#)
 1. [The PSF of the Mirror Units](#)
 2. [The PSF of the Detector](#)
 3. [PSF correction factor](#)
 12. [Burst Length corrections](#)
5. [Symbols and quantities used in formulae](#)
6. [References](#)

[\[Home\]](#) [\[ToC\]](#) [\[Previous\]](#) [\[Next\]](#) [\[Down\]](#)

The MECSicans

The Medium Energy Concentrator Spectrometer team has evolved during the various phases of the SAX project. Some persons formerly involved even in a key role, like the latest Experiment Investigators [G.Boella](#), [S.Re](#) and [G.Conti](#), have now happily (👍) moved to other projects or institutions, while other persons, engaged from the beginning or at a later stage, are at present (Feb 98) still active (👍) and busy (👎).

The team includes mainly staff of two CNR institutes : [IFCTR](#) in Milan and [IFCAI](#) in Palermo.

We list here all people in alphabetic order according to the "busy flag".

- 👎 [Lucio Chiappetti](#) ([IFCTR](#))

is the current MECS analysis software responsible. He has assisted the E.I. for the on-board operating modes, and participated to other SAX mission activities. He has participated to the organization of the ground calibration campaign, to the commissioning phase, and to the relevant analysis.

- 👎 [Giancarlo Cusumano](#) ([IFCAI](#))

follows the analysis of the ground and flight calibrations, with particular regard to the optics effective area.

-  **Stefano Del Sordo (IFCAI)**

follows the analysis of the ground and flight calibrations, with particular regard to the modelling of the detector unit.

-  **Cettina Maccarone (IFCAI)**

follows the analysis of the ground and flight calibrations, and other SAX mission activities, with particular regard to the data and s/w organization. She has participated to the ground calibration campaign, to the commissioning phase, and to the relevant data analysis organization.

-  **Teresa Mineo (IFCAI)**

follows the analysis of the ground and flight calibrations, with particular regard to anything which concerns the response matrix. She is assembling together all contributions in the matrix generation program.

-  **Silvano Molendi (IFCTR)**

participated to the ground calibration campaign and to the commissioning phase, and follows the analysis of the ground and flight calibrations, with particular regard to the optics point spread function.

-  **Bruno Sacco (IFCAI)**

is the current MECS calibration responsible. He has been involved in the Mirror Unit development since early phases (in particular for the ray tracing program), supports the project as IFCAI director, participated to the ground calibration campaign and to the analysis of the ground and flight calibrations.

-  **Chris Butler (ASI)**

has been the SAX Payload Manager, and is the present BeppoSAX Flight Director and he has to be considered as MECS Team ad honorem member for his unvaluable support in all the MECS activities.

-  **Giancarlo Conti (IFCTR)**

has been the Optics Experiment Investigator during the development phase, has followed the development of the Mirror Units and their integration on the satellite, has participated to the organization of the ground calibration campaign, to the commissioning phase, and to the relevant analysis.

-  **Giovanni La Rosa (IFCAI)**

has followed the development of the GSPC detectors and their integration on the satellite, has participated to the entire ground calibration campaign, to the commissioning phase, and to the relevant analysis.

-  **Giuliano Boella**

([University of Milan](#), and formerly IFCTR) has been the MECS Experiment Investigator for the overall experiment during the entire development phase (beside being the SAX Project Scientist, and the former IFCTR director).

-  **Giuseppe Bonelli (IFCTR)**













participated to earlier work on the optics side.

-  **Angelo Bonura**

(formerly at IFCAI) participated to earlier work on the detector side.

-  **Filippo Celi (IFCAI)**

participated to earlier work on the detector side.

-  **Oberto Citterio**
(formerly at INFN and IFCTR, presently at [Merate Observatory](#)) has developed the electroforming techniques for X-ray optics, which is now being employed also for Jet-X and XMM.
-  **Paolo Conconi (Merate Observatory)**
participated to earlier work on the optics side.
-  **Renato Di Raffaele (IFCAI)**
participated to earlier work on the detector side.
-  **Fabrizio Giambertone**
(formerly at IFCAI) maintained the local SAX s/w systems and data archive.
-  **Salvo Giarrusso (IFCAI)**
supported Peppino Manzo and Stefano Re in an early phase of the detector development.
-  **Luigi Lombardo**
(formerly at IFCAI) participated to earlier work on the detector side.
-  **Peppino Manzo**
(formerly at IFCAI, presently at ITESRE) has been Detector Experiment Investigator in an early phase, before swapping his role with Stefano Re as HP-GSPC E.I..
-  **Enrico Mattaini (IFCTR)**
has played a key role in the manufacturing of the prototypes of the Mirror Units, the finalization of the electroforming technique, and all mechanical aspects.
-  **Stefano Re**
(formerly at IFCAI) has been the latest Detector Experiment Investigator in charge during the development phase, has followed the development of the GSPC detectors and organized the ground calibration campaign at Panter.
-  **Emilio Santambrogio (IFCTR)**
supported Enrico Mattaini in the development of the Mirror Units.
-  **Giorgio Sironi (University of Milan)**
participated to earlier work on the detector side.
-  **[Mario Tripiciano](#) (IFCAI)**
participated to the ground calibrations and managed the local SAX Computer System.

[\[Home\]](#) [\[ToC\]](#) [\[Previous\]](#) [\[Next\]](#)

A guided tour to the MECS and to its response matrix

This set of HTML pages has been written by [Lucio Chiappetti](#) ([IFCTR](#))
with substantial input from the entire [MECS team](#),

and in particular by [Teresa Mineo](#) and [Cettina Maccarone](#) (IFCAI).

*. [Table of Content](#)

Navigation through the tour is possible in an ordered way using the [Table of Content](#), or the activated navigation "buttons" at the end of each page, or randomly just following the links or clicking on images.

1. Introduction

We give here a quick description of the Medium Energy Concentrator Spectrometer (MECS) [1] on board [the BeppoSAX satellite](#). In particular we give some information on the content of the various [calibration files](#), their meaning and role (with particular, but not exclusive, regard to those entering the generation of the response matrix).

All values (even those inlined in the text, or plotted) will be produced on-line from the latest calibration files, in order to guarantee an automatic update.

Note that, for plots produced by IDL, we cannot guarantee availability of a free license at all times. If a plot cannot be produced, please try later.

1.1 MECS interactive map

The MECS consists of three units (hereafter named M1, M2, and M3), each composed of a grazing incidence Mirror Unit (MU), and of a position sensitive Proportional Counter (GSPC) located at the focal plane. The MUs are connected to the GSPCs by a carbon fiber envelope, ~2 m long.

The following interactive map gives an impression of the components of one MECS unit. You may click on the various items and labels to access information about [the MECS components](#) or [the MECS calibration parameters](#).

Note that the vertical scale is magnified by about a factor 8 and some items have been exploded from their actual position for clarity. The carbon fiber optical envelope connecting mirrors and detector is not shown.

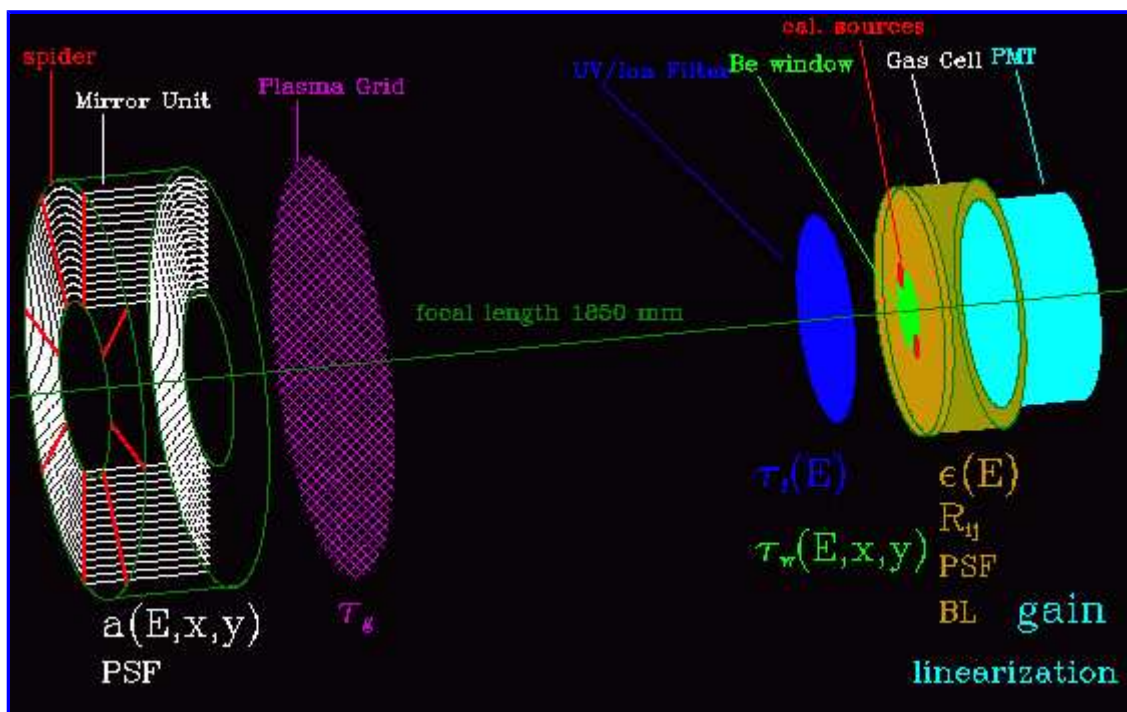


Fig. 1.1-I : MECS interactive map

1.2 The response matrix : introduction

The response matrix of an X-ray detector allows to reconstruct source photon spectra from the observed counts (counts per Pulse Height Analyser [PHA] or Pulse Invariant [PI] channels). The detected count spectrum is in fact given by the convolution of the actual photon spectrum by the

response matrix:

$$C_i = \int_0^{\infty} \frac{dN}{dE} R(i, E) dE = \sum_j \frac{dN}{dE}(E_j) R_{ij} \Delta E_j = \sum_j S(E_j) Q_{ij} \quad (1)$$

[Click on each formula element to see its dimensions (physical units)]

where C_i are the detected counts in the i -th PI channel dN/dE is the photon input spectrum, R is the overall response matrix and j runs on a discrete binning of the photon input energy E , each j -th bin with ΔE_j width.

In formula (1) the matrix Q_{ij} corresponds to the XAS-format matrix file and has dimensions of [cm² keV] however it is customary to use R_{ij} as overall response matrix and to decompose it in two terms :

$$R_{ij} = P_{ij} A(E_j) \quad (2)$$

where:

- P_{ij} is the redistribution matrix (the adimensional probability that a photon of input energy E_j is detected in channel i) which correspond to an OGIP RMF file
- the 1-d array $A(E_j)$ is the total effective area has dimensions of an area [cm²] and includes all contributions which depend only on the input photon energy and corresponds to an OGIP ARF file. For the MECS this is the overall effective area.
- (in the case of the MECS there are no terms which depend on the PHA/PI channel only)

1.2.1 Calibration data contributing to the redistribution matrix

The following (conventional or real) components enter in the computation of the response matrix :

- the (conventional) input photon [energy grid](#) E_j
- the [channel boundaries](#) of the PI channels given by the [gain relation](#)
- the [energy resolution](#) in turn described by
 - a [Gaussian component](#) G
 - a [non-Gaussian low energy tail](#) T
- the [escape fractions](#) of fluorescence photons (they must be taken into account both in the gain relation as well as in the computation of the response (the matrix is the sum of unescaped and escaped components))

The overall redistribution matrix can therefore be obtained as a sum of several terms (click on each formula component for details) as indicated below. Index k runs on the four main Xenon escape peaks.

Note that not all terms are defined in all energy ranges.

Also probabilities G and T are appropriately normalized for [escape fractions](#) in such a way that the total probability of a photon of energy E_j to spread over all channels is unity (except close to the extrema of the energy range where a photon may be lost out of the useful range).

$$P_{ij} = P_i(E_j) = G_i(E_j) + T_i(E_j) + \sum_{k=1}^4 G_i(E_j - E_k) + T_i(E_j - E_k) \quad (3)$$

A [flow-chart](#) of the calculation if the RMF in the [XAS MECS matrix accumulation program](#) is given in [Fig. 1.2.1-I](#)

1.2.2 Calibration data contributing to the overall effective area

The effective area as a function of energy is the product of several array or scalar terms. Some of these terms also depend on other parameters, like the position on the detector ,or the burst length limits.

$$\mathbf{A}(\mathbf{E}) = \mathbf{a}(\mathbf{E}, \mathbf{x}, \mathbf{y}) \tau_g \tau_f(\mathbf{E}) \tau_w(\mathbf{E}, \mathbf{x}, \mathbf{y}) \varepsilon(\mathbf{E}) \mathbf{f}(\mathbf{E}, \mathbf{r}) \mathbf{b}(\mathbf{E}, \mathbf{B}_1, \mathbf{B}_2) \quad (4)$$

The terms entering the above formula (click on each factor to access relevant information) are :

- the [mirror effective area](#)
- the [transmission of the plasma suppression grid](#)
- the [transmission of the Kapton or Lexan filters](#)
- the [transmission of the Beryllium window](#)
- the [detector quantum efficiency](#)
- a correction for the [fraction of PSF](#) falling in the region in which the spectrum has been accumulated
- a correction for the [Burst Length range](#) in which the spectrum has been accumulated

A [flow-chart](#) of the calculation if the RMF in the [XAS MECS matrix accumulation program](#) is given in [Fig. 1.2.2-1](#)

1.3 Calibration data used in event linearization

The position and energy of a photon are computed by the [Electronics Unit](#) based on the output of the [PMT](#). This process introduces distortions both in position and gain because of three effects :

- spatial disuniformity of the [PMT gain](#) (energy independent)
- different viewing angles of different scintillation positions (energy independent)
- curvature of the [Be window](#) with associated distortion of the electric field (energy dependent)

The relevant distortions have been modelled using ground measurements based on a [multipinhole mask](#) ; the modeling is given as a [relation](#) converting unlinearized x,y pixel positions into linearized X,Y positions in mm, and as a [map](#) to correct for the position dependency of the gain. Moreover, variations in the detector temperature produce slightly changes in the gain that are corrected with respect to an [absolute reference](#).

There are a number of calibration parameters that are typically used in [corrections performed during data accumulation](#). We give here a quick reference list, with pointers to details kept elsewhere :

- the [coefficients](#) used for linearization of photon positions
- the [maps](#) to correct for the gain [positional dependency](#)
- the coefficients to correct for the gain [time \(temperature\) dependency](#)

The final effect of the gain corrections is to convert PHA channels into PI channels.

1.4 Other calibration data

There are a number of calibration parameters which do not enter in the computation of the response matrix or in the corrections performed during data accumulation, but useful for the attitude reconstruction and data analysis. We give here a quick reference list, with pointers to details kept elsewhere :

- the MU+Detector [misalignments](#) used to relate pixel to celestial positions
 - the gain and positional [reference](#) of the built-in [calibration sources](#)
-

1.5 MECS background

An invited paper [3] discussing the current knowledge of the analysis about the instrumental and cosmic background observed by the MECS has been presented at the RXTE/BeppoSAX Lincei conference "The Active X-ray sky" in Rome, 21-24 Oct 1997 (see preprint in [astro-ph/9712251](#) or locally a [preview](#))

The reader is referred to such paper for details. There are at present no standard XAS calibration files related to the background, although some material has been released by SDC. We recall here only the most important issues.

The background observed by the MECS is constituted by several components :

- the instrumental background, in turn comprising
 - the noise of the [PMT](#) in the lowest channels, below the useful energy range
 - a gently sloping [plateau](#) continuum below 4 keV and another plateau at an higher level above 4.5 keV, terminate by the high energy cutoff whose precise position (> 10.5 keV) depends on the [gain setting](#)
 - a small feature [between 4 and 4.5 keV](#), attributed to fluorescence photons of events lost

- by attachment (indicated with number 6 in the [figure](#) of the event interaction in a [GSPC](#))
 - a line feature peaked around the ^{55}Fe energy of the [calibration sources](#). This component is position dependent, and is attributed to calibration events assigned the wrong position (indicated with number 5 in the [figure](#) of the event interaction in a [GSPC](#)) and therefore corrected with the wrong [gain correction](#) (whence the broadening of the feature)
 - some minor features, present only in the bright Earth spectra, attributed to Sun albedo or atmospheric fluorescence
- the cosmic background, whose description is beyond the present scope, but which is affected by the following calibration effects :
 - the [vignetting](#) of the optics
 - the positional dependency of the [infinity correction](#)
 - the spatial modulation of the [Be window transmission](#)

For the above reasons, it may not be wise to use as background subtraction the naive method of extracting gross source counts from a small circular region, and subtracting the background from a surrounding annulus. In fact the spectrum of the annulus is likely to be affected by the following effects :

- a non negligible [fraction of the PSF](#) of the source (a few percent) may be contaminating it
- the cosmic contribution will be underestimated because of vignetting effects
- the [residual calibration events](#) may be higher than in the detector centre

For these reasons it is advisable to subtract a blank field background accumulated in the same region where the source is extracted.

[\[Home\]](#) [\[ToC\]](#) [\[Previous\]](#) [\[Next\]](#)

2. The MECS components

The Medium Energy Concentrator Spectrometer (operating in the energy band 1.3-10 keV) is composed by three nearly identical units (named M1, M2, M3) sharing a common [Electronic Unit](#) (EU).

Each MECS unit (Field of View of 28' radius and angular resolution at the arcmin level) is composed by two major parts:

- a [Mirror Unit](#) (MU)
- a [Detector Unit](#) (DU)

Unfortunately, since 6 May 1997, unit M1 is no longer operating due to a failure in the electronic equipment (power supply).

2.1 Mirror Unit

The MU is connected to the DU by a carbon fiber envelope (there are actually two envelopes, one containing M2 and M3, and the other one M1 and the LECS. The carbon fiber envelopes are mounted on the spacecraft optical bench, to which also the other SAX instruments are connected.

The [misalignments](#) of the MU optical axes w.r.t. the spacecraft axes have been calibrated in flight using [some raster scan observations](#).

2.1.1 The mirrors

Each MU is composed by 30 nested coaxial and confocal grazing incidence mirrors in a double cone configuration (the [exploded view](#) shows only 10 shells for clarity). A fourth identical MU is used in front of the LECS detector.

The mirrors have a double cone geometry to approximate the Wolter I configuration (paraboloid-hyperboloid), with characteristics listed here below. The MU design was optimized to have the best response at 6 keV. A replica technique by nickel electroforming from super-polished mandrels was used to build up the mirrors. A 1000 Å thick gold layer provides the X-ray reflecting surface.

MU characteristics

Geometry	double cone (paraboloid-hyperboloid)
Number of nested mirrors	30 (coaxial, confocal)
Grazing incidence angles:	
- outermost mirror	0.62°
- innermost mirror	0.25°
Mirror diameter	from 68 to 162 mm
Mirror overall length	300 mm
Mirror thickness:	
- 10 inner mirrors	0.2 mm
- 10 medium mirrors	0.3 mm
- 10 outer mirrors	0.4 mm
Mirror material	nickel (electrodeposited)
Reflecting surface:	
- material	gold (evaporated)
- roughness	< 10 Å
Focal length	1850 mm
Geometric collecting area:	
- per MU unit	123.9 cm ²
Case and spiders material	stainless steel
Mirror Unit weight	13 Kg

The mirror units calibration parameters are the [effective area](#) and the [Point Spread Function](#). The MU effective area has been calibrated at the Panter facility and it constitutes the only on-ground effective area measurement.

2.1.2 The spider

The mirror shells are held together by two eight-arm spiders. Their shadow is clearly visible when observing very bright sources. The ~9% reduction in geometric area due to the spider obscuration is implicitly taken into account in the [mirror effective area](#)

2.1.3 The Plasma suppression grid

An Au-coated Tungsten grid located behind the Mirror Units and kept at +28 V shields the [Be entrance window](#) of the detector from (charged) plasma particles.

Its calibration parameter is the relevant [transmission](#)

2.2 Detector Unit

2.2.1 The ion shield and UV filter

A (passive) filter, placed in front of the detector entrance window, is used both to stop high velocity charged particles passing through the plasma grid, and to stop UV photons. The three MECS units carry different filters :

- a Kapton + Al filter in front of M1
- a Lexan + Al filter in front of M2 and M3

Their calibration parameters are the relevant [transmissions](#)

2.2.2 The gas cell

The detector is a [GSPC](#) (Gas Scintillation Proportional Counter), constituted by a 96 mm diameter ceramic chamber filled with Xenon. One can subdivide it in the following components :

- a front cover holding two radioactive ⁵⁵Fe [calibration sources](#)
- the 30 mm diameter entrance [Beryllium window](#), kept at a voltage of about -8000 V
- a 20 mm thick [drift region](#), separated by
- a grid kept at a voltage of about -7000 V from
- a 175 mm thick [scintillation region](#) ending with
- the 80 mm diameter quartz exit window to which is attached
- the [Photo Multiplier Tube](#)

The [principles of operation of a GSPC](#), together with a close view of the MECS Detector Unit (and its [characteristics](#)) are recalled elsewhere. The relevant calibration files are also listed [there](#), as well as below under individual sub-components.

The voltage setting of the Be window and drift/scintillation grid and of the PMT may affect the gain and resolution parameters. Note however that these values are kept fixed at the nominal values (to which all ground and flight calibrations refer).

The PMT nominal HV setting used during ground calibration and first light was changed in flight before the begin of the Performance Verification phase.

2.2.2.1 The calibration sources

Two radioactive iron (^{55}Fe) calibration sources are located in containers on the top cover of the gas cell, on two diagonally opposite positions on the edge of the sensitive part of the Field of View. They supply the primary source for the gain monitoring and their energy (5.894 keV) is assumed as primary gain normalization reference.

2.2.2.2 The Be window

The 50 micron Beryllium window is supported by a thicker strongback (shown in figure below) in form of a circular ring and four ribs. It delimits the sensitive part at the centre of the Field of View.

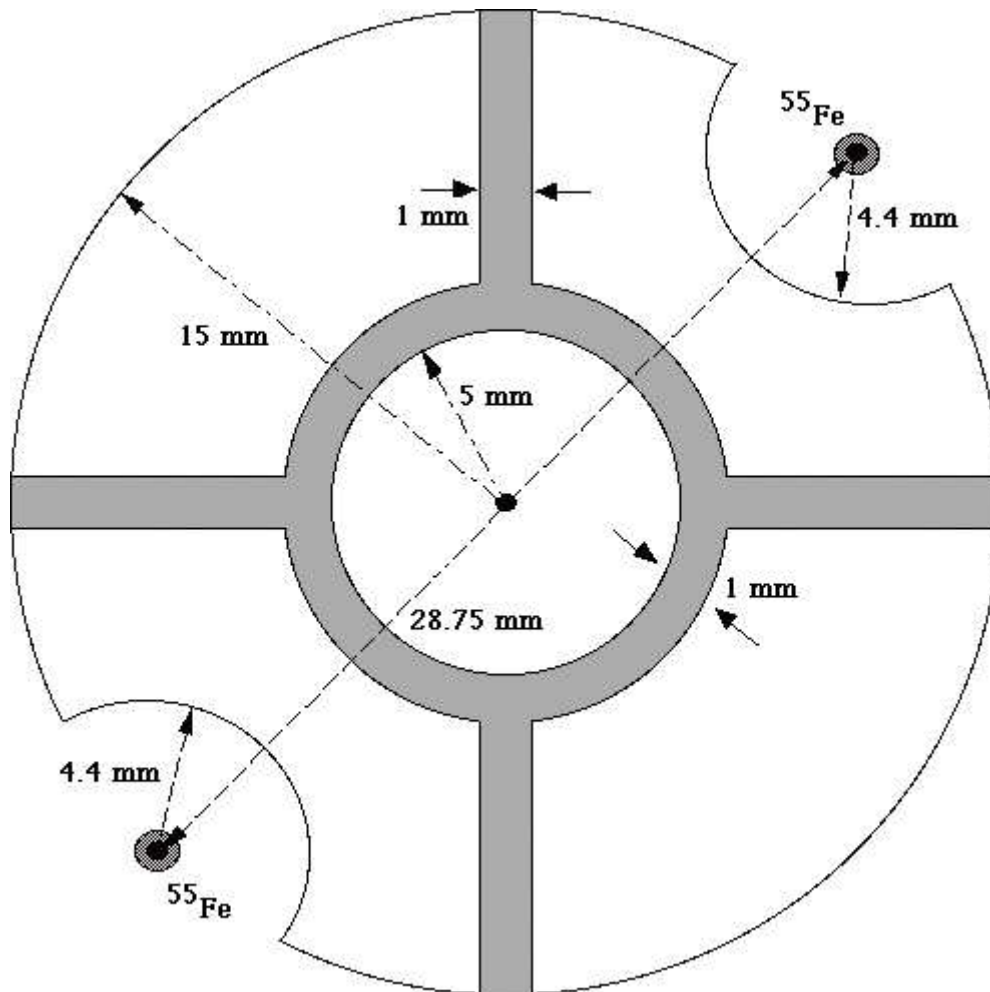


Fig. 2.2.2.2-I : geometrical characteristics of the Be window and strongback

Its calibration parameter is the relevant transmission, which is function both of energy (being the prime responsible of the low energy cutoff in the effective area), and position (because of the presence of the strongback). The effect of the strongback is its geometrical shadow convolved through the detector PSF.

2.2.2.3 The drift region

The drift region is the primary region where the X-ray photons interact with the gas and liberate an electron cloud which then drifts towards the -7000 V grid.

The calibration parameters due to this region are

- the relevant quantum efficiency
- the energy resolution
- the escape fraction
- the detector PSF

2.2.2.4 The scintillation region

In this region the electron clouds scintillate giving rise to bursts of UV light via interaction with the

Xenon ions. This region contribute also to the total efficiency especially for hard X-ray photons. However, the energy of events interacting there cannot be reconstructed. They are then rejected by Burst Length selection.

The calibration parameters due to this region are the relevant [quantum efficiency](#) and the [Burst Length](#) related corrections.

2.2.3 The Photo Multiplier Tube

The Hamamatsu position sensitive PMT, with 15 dynodes and a crossed-wire anode, is operated at about 1000 V. For each burst of light corresponding to a detected photon it gives rise to the signals processed by the [EU](#) to measure arrival time, energy and position of photons.

The PMT setting and behaviour affects several calibration parameters :

- its voltage setting is the main contribution to the absolute [gain setting](#). It has been changed during the Commissioning Phase (with respect the on ground calibration settings) to optimize the coverage of the 1-10 keV range over the entire Field of View
- the nonuniformities in the entrance window and in the electrode arrangement are responsible of the [positional gain dependency](#)
- the sensitivity of the PMT to ambient temperature is responsible of the variations of [gain with time](#)
- nonuniformities in the electrodes are responsible of the [geometrical distortion](#)

2.3 Electronics Unit

The Electronics Unit consists of :

- (2.3.1) the Front End Electronics receives the signals from the PMT (a trigger, the digitized energy, or PHA, and four raw position signals). It reconstructs the event X,Y position and generates the [Burst Length](#) and arrival time information, and places everything in a FIFO register. It also performs some event qualification (taking account of valid and rejected events in [ratemeters](#) named `trigger`, `valemin`, `valblmin`, `rejemax` and `rejblmax`).
- (2.3.2) the Event Processor reads the events from the FIFO, and performs some (software) rejection based on programmable E, BL and XY thresholds. In case of high rates some events may be lost if the microprocessor is busy. All these losses are counted and are available in [ratemeters](#) named `rejmbus`, `reje`, `rejbl`, and `rejxy`.
- ((2.3.3) the Communication Processor is responsible of assembling event data into scientific [telemetry packets](#), and ratemeter data into engineering [telemetry packets](#). In case of high rates it is possible that the buffer space for scientific packets fills up : the information on the total number of lost events and the non-transmission interval is available in the header of the first packet transmitted afterwards.

[\[Home\]](#) [\[ToC\]](#) [\[Previous\]](#) [\[Next\]](#)

3. Principles of operation of the ME-GSPC

The focal plane detectors are Xenon filled GSPC (Gas Scintillation Proportional Counters), working in the range 1.3-10 keV with an energy resolution of ~8% at 5.9 keV and a position resolution of ~0.5 mm (corresponding to 1 arcmin, approximately) at the same energy.

The [gas cell](#) is composed by a cylindrical ceramic body (96 mm internal diameter) closed, at the top, by a 50 micron thick entrance [Beryllium window](#) with 30 mm diameter and, on the bottom, by an UV exit window made of Suprasil quartz with 80 mm diameter and 5 mm thickness, as schematically shown in fig. 3-I below.

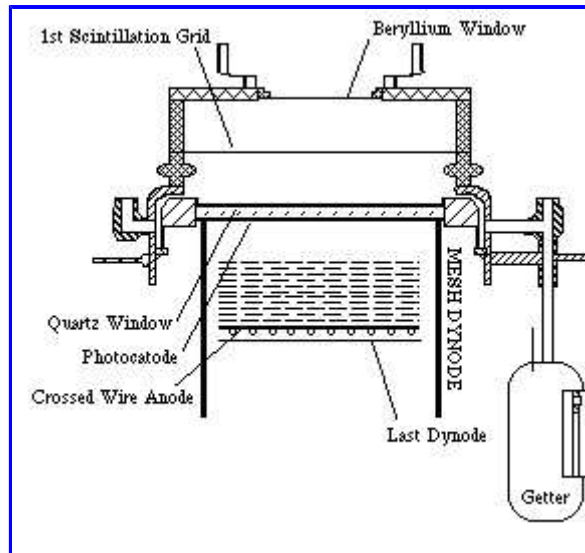


Fig. 3-I : click-sensitive scheme of the MECS GSPC

A typical GSPC operates as follows (see also [fig. 3-II](#)):

An X-ray photon absorbed in the [gas cell](#) liberates a cloud of electrons. A uniform electrical field across the cell [drifts](#) the cloud up to the [scintillation region](#), with an higher electric field, where UV light is produced through the interaction of the accelerated electrons with the Xe ions.

The amplitude of the UV signal, detected by a [photomultiplier](#) (PMT), is proportional to the energy of the incident X-ray. The duration of the signal, the so-called Burst Length (BL), depends on the interaction point and it is used to discriminate genuine X-rays against induced background events. BL rejection may be carried out on board and/or on-ground. The BL rejection mechanism on board is based on a programmable BL acceptance window (not energy dependent).

Two grids inside the cell separate the absorption/ [drift region](#) (20 mm depth) from the [scintillation region](#) (17.5 mm depth). The UV readout system consists of a crossed-wire anode position sensitive [Hamamatsu PMT](#) with quantum efficiency of ~20%.

The high voltage nominal values are respectively -8 kV for the Be window -7,kV for the scintillation grid, while for the PMT of M1 M2,,and M3 units the ground settings at Panter were 1000, 992, and 943 V. These settings were used also in flight during the first light observations, but were updated just before the start of the commissioning phase to the present values of 979, 976 and 926 V

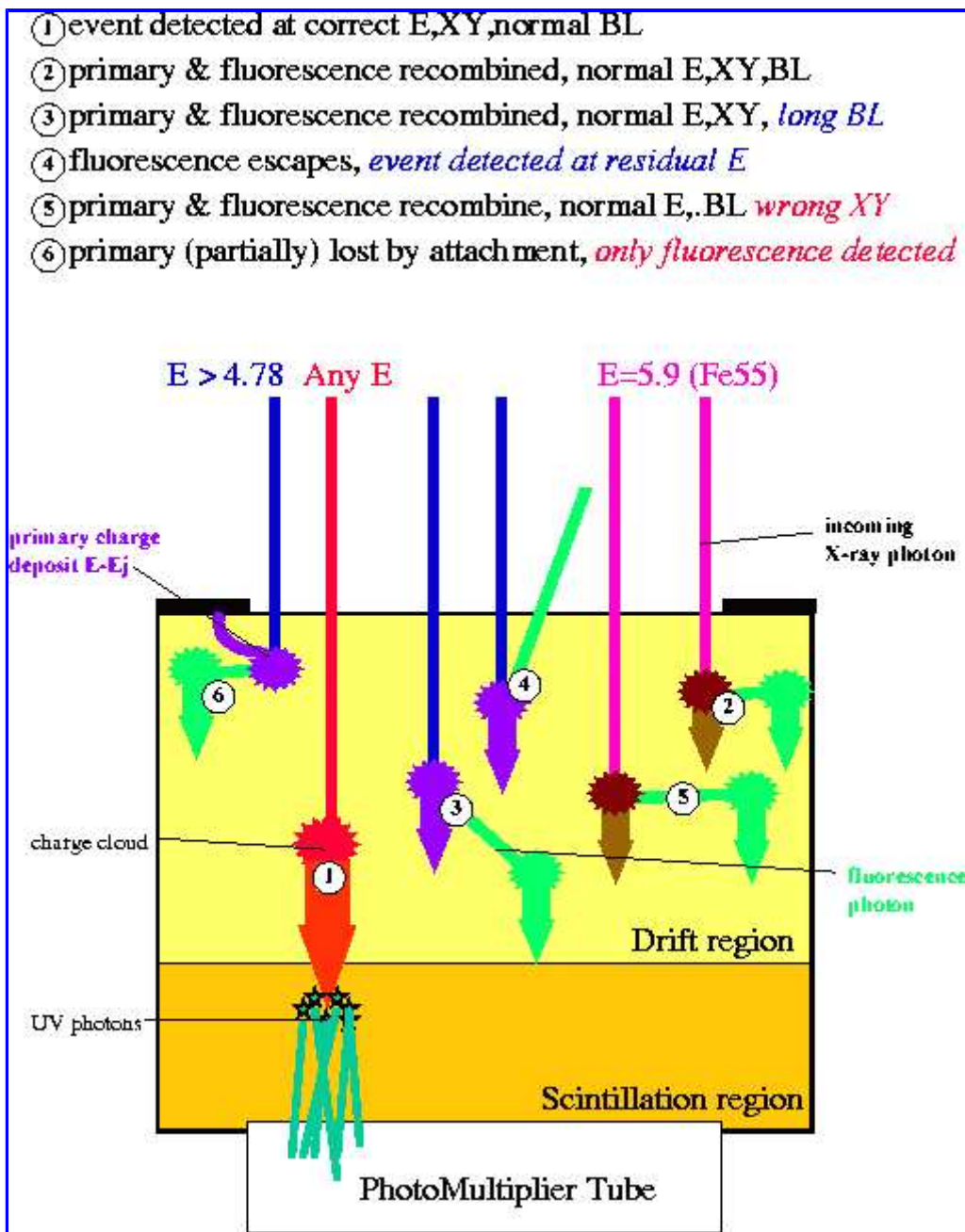


Fig. 3-II : photon interactions in the MECS GSPC

The entrance window is externally supported by a Beryllium [strongback](#) structure, 0.55 mm thick, consisting of a ring (10 mm inner diameter, 1 mm width) connected to the window border by four ribs.

Two ^{55}Fe collimated [calibration sources](#) (line at 5.894 keV), with an emission rate of ~ 1 count per second, are located, diametrically opposed, near the edge of the [Be window](#). These sources, continuously visible at the edge of the Field of View (FOV), allow the monitoring of the detector [gain](#). Furthermore, a [passive ion shield](#) is placed in front of the detector.

GSPC detector characteristics are listed here below.

GSPC characteristics

Operative range	1.3 - 10 keV
Energy resolution	$\sim 8\%$ at 5.9 keV
Position resolution	~ 0.5 mm (~ 1 arcmin)
Gas cell geometry:	
- internal diameter	96 mm
UV exit window:	
- material	Suprasil quartz
- diameter	80 mm
- thickness	5 mm
Gas type	Xenon
Gas filling pressure	1.0 atm at 25 °C
X-ray window:	
- material	Beryllium

```
- diameter          30 mm (FOV 56' diameter)
- thickness         50 um
- central region    10 mm diameter
X-ray window strongback:
- material          Beryllium
- thickness         0.55 mm
- width            1 mm
```

[\[Home\]](#) [\[ToC\]](#) [\[Previous\]](#) [\[Next\]](#)

4. The MECS calibration parameters

The Medium Energy Concentrator Spectrometer calibration parameters used by the [XAS](#) software reside in files in the [\\$XASTOP/calib/sax/mecs](#) directory, while those used by the [SAXDAS](#) software have been generated from the master XAS version.

We give here a reference to each calibration parameter, with indications of

- its physical meaning, and in which [hardware component](#) it originates
 - its current values
(inclusive of GIF plots : note that such plots are generated on the fly and survive for 1 minute ; in case of problems RELOAD the HTML file and RELOAD IMAGES as well)
 - how it has been calibrated
 - in which file(s) it resides
-

4.0.1 Input photon energy grid

The input energy grid used in the computation of the response matrix can in principle be any grid of appropriate spacing. The current version of the MECS response matrix software uses an equispaced grid (hardcoded) of 1160 bins from 0.4 to 12 keV, each bin is 0.01 keV wide.

4.1 Mirror effective area

The effective area of the [optics](#) is given by the product of three components.

- [the on-axis area](#)
- [the vignetting correction](#)
- [the correction to infinity](#)

4.1.1 On-axis area

The on-axis area of the optics is tabulated as a function of energy in calibration files

`m{1,2,3}_onaxis.area`

It has been calibrated on ground using various energies at the Panter calibration facility [with the Mirror Units](#) in the beam and without them (so called [flat fields](#)). The experimental results have been matched to the theoretical prediction (geometric area and gold reflectivity according to Henke 1983) by an ad-hoc second order polynomial.

A further adjustment (mainly around 2 keV) was made in flight using the Crab nebula spectrum.

The on-axis area (which corresponds to the Panter observing conditions, i.e. a point source at a finite distance of 130 m) is plotted here below.

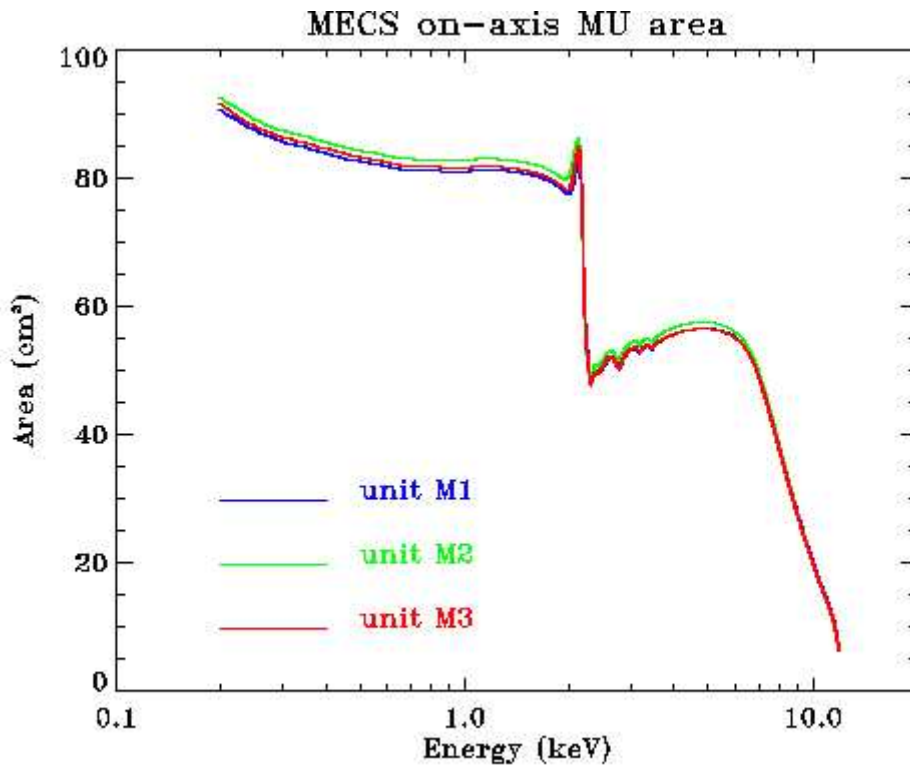


Fig. 4.1.1-I : MECS optics on-axis area

[\[Home\]](#) [\[ToC\]](#) [\[Previous\]](#) [\[Next 4.1.2 cont.\]](#)

[continues from [4.1.1](#)]

4.1.2 Vignetting correction

The off-axis optics area (at an angle theta from the optical axis) is obtained by multiplying the on-axis area for a vignetting correction which has also been originally calibrated on the ground, and revised according to Crab observations and is interpolated as a function of energy from a set of coefficients.

Coefficients are kept in files `m{1,2,3}_vignetting.coeff`.

The coefficients give the vignetting correction as a function of the off-axis position r in mm according to the following formula :

$$V(r, E) = (1 + V_1(E) \cdot r + V_2(E) \cdot r^2)^{-1}$$

The conversion between r and theta (e.g. in arcmin) is given by the optics [platescale](#). In the figure below the vignetting correction at different energies is reported as a function of theta.

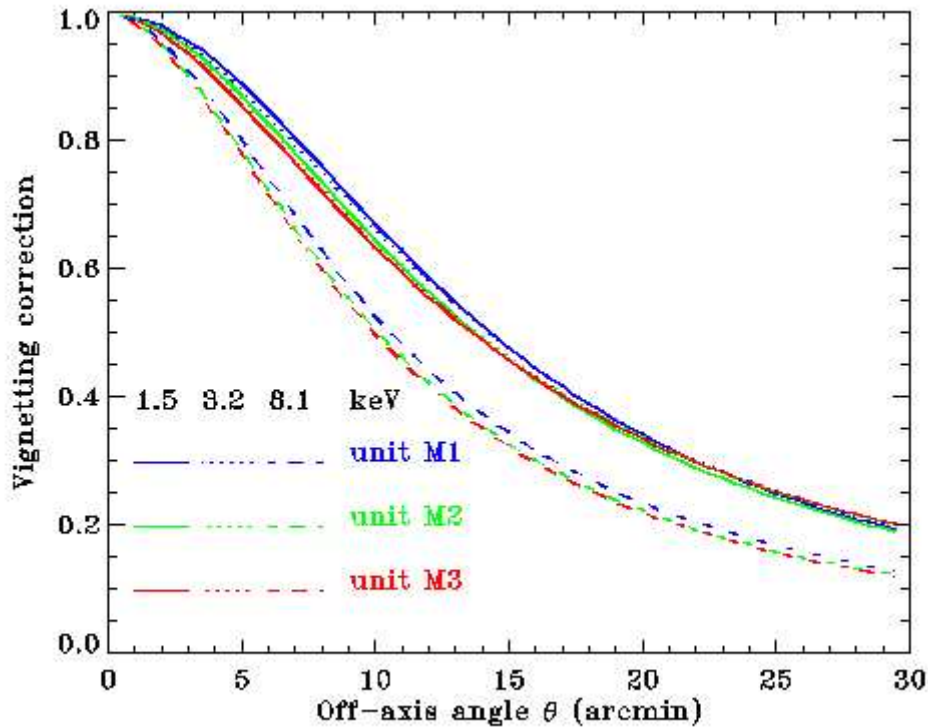


Fig. 4.1.2-I : examples of MECS vignetting correction as a function of off-axis angle for the three MECS units, and for three energies (1.5, 3.2 and 8.1 keV)

Additional representations (as separately numbered figures) can be obtained via the following form :

Plot/compute vignetting correction V for MECS unit :

select ONE type of data representation, the relevant value and data format

V(theta) at given E

keV

V(E) at given theta

arcmin

V(x,y) image at E

keV

[\[Home\]](#) [\[ToC\]](#) [\[Previous\]](#) [\[Next 4.1.3 cont.\]](#)

[continues from [4.1.2](#)]

4.1.3 Infinity correction

A further correction is necessary to reduce the measurements done at Panter at a finite source distance of 130 m (divergent beam) to the flight condition of sources at infinity (parallel beam). The correcting coefficients have been derived by comparison of ground measurement with results of a ray tracing code. As such they are the same for all 3 MECS units.

The correcting factor is interpolated as a function of energy and off-axis angle theta from a set of coefficients kept in file [panter.infinity](#).

The coefficients correspond to a cubic polynomial in theta.

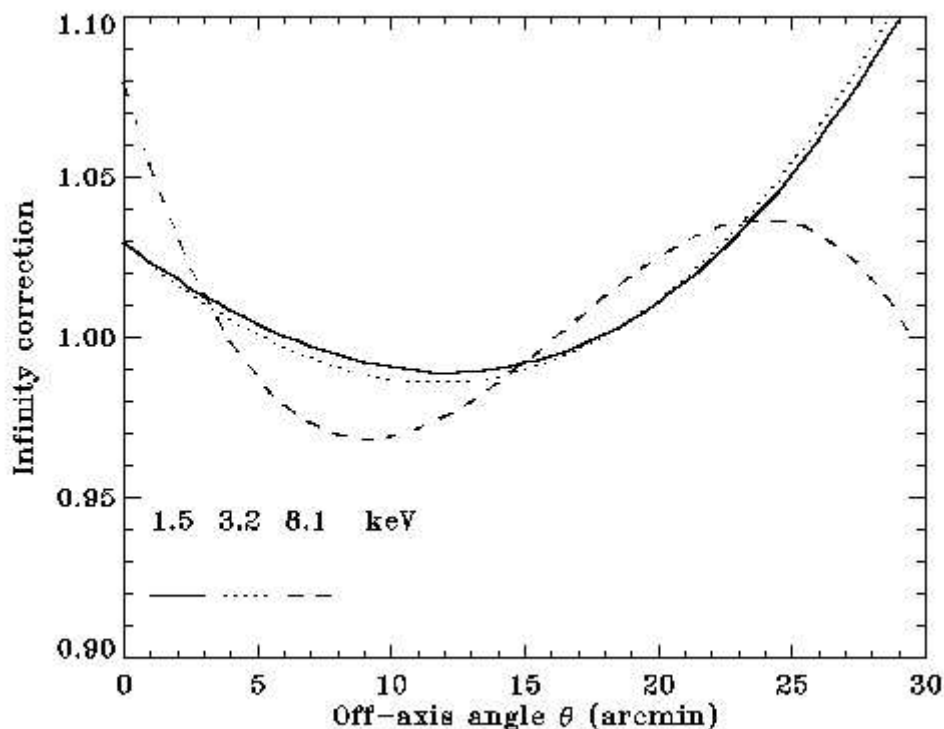


Fig. 4.1.3-I : examples of the Panter-to-infinity correction as a function of off-axis angle for three energies (1.5, 3.2 and 8.1 keV)

Additional representations (as separately numbered figures) can be obtained via the following form, inclusive of the overall vignettted area (compound calibration parameter, given by the product of the various corrections) :

Plot/compute ONE of the following parameters for MECS unit

Quantity v	Symbol	Select
Infinity correction (unit-independent) I	I	<input checked="" type="radio"/>
Vignetting correction	V	<input type="radio"/> (see section 4.1.2)
On-axis area	A	<input type="radio"/> (see section 4.1.1)
Vignettted area (at finite distance)	A*V	<input type="radio"/>
Positional correction	V*I	<input type="radio"/>
Vignettted area at infinity	A*V*I	<input type="radio"/>

select ONE type of data representation, the relevant parameter and data format

- v(theta) at given E keV
- v(E) at given theta arcmin
- v(x,y) image at E keV

4.1.4 Focal length

The focal length of the mirrors is 1850 mm, which corresponds to a platescale (value read from provisional calibration file `mir.dat`) of 111.44 arcsec per mm in the focal plane. The correspondence between mm and image pixels depends on the choice of the linearized pixel size during the linearization procedure. The unlinearized pixel sizes close to the detector centre are the average of the 3rd and 4th linearization coefficient in file `m{1,2,3}_xy.coeff`:

- for M1 .17141 mm (average of .17600 on x and .16682 on y)
- for M2 .16326 mm (average of .16354 on x and .16298 on y)
- for M3 .17509 mm (average of .17561 on x and .17458 on y)

[\[Home\]](#) [\[ToC\]](#) [\[Previous\]](#) [\[Next 4.1.5 cont.\]](#)

[continues from [4.1.4](#)]

4.1.5 Misalignments

The misalignments between the spacecraft axes XYZ and the detector axes of each MECS unit xyz can be defined by three angles as follows :

- the spacecraft axes are defined with the Z axis being the NFI pointing axis, the Y axis being parallel to the solar array, and the X perpendicular to it, as shown in the [payload accomodation](#) figure.
- the detector xy mechanical axes are defined by its mechanical mount and are parallel to the [strongback](#) axes and to the detector electronic axes (i.e. [linearised](#) pixel coordinates)
- the detector z axis completes the triad, and is the axis along the [gas cell](#) and [mirror unit](#) axis. The DU and MU mounting is solidal because of the carbon fiber envelope, and the misalignments are due to its mounting on the spacecraft optical bench.
- the first angle alpha corresponds to a rotation around the Z axis (rotations must be applied in this order)
- the second angle beta corresponds to a rotation around the y' axis
- the third angle gamma corresponds to a rotation around the x'' axis
- the effect of the three rotations is shown in [fig. 4.1.5-I](#)
- the mechanical orientation of the three MECS detectors is such that unit M3 xy axes are grossly parallel w.r.t. the spacecraft XY axes, while unit M1 and M2 axes are flipped (see [fig. 4.1.5-II](#))

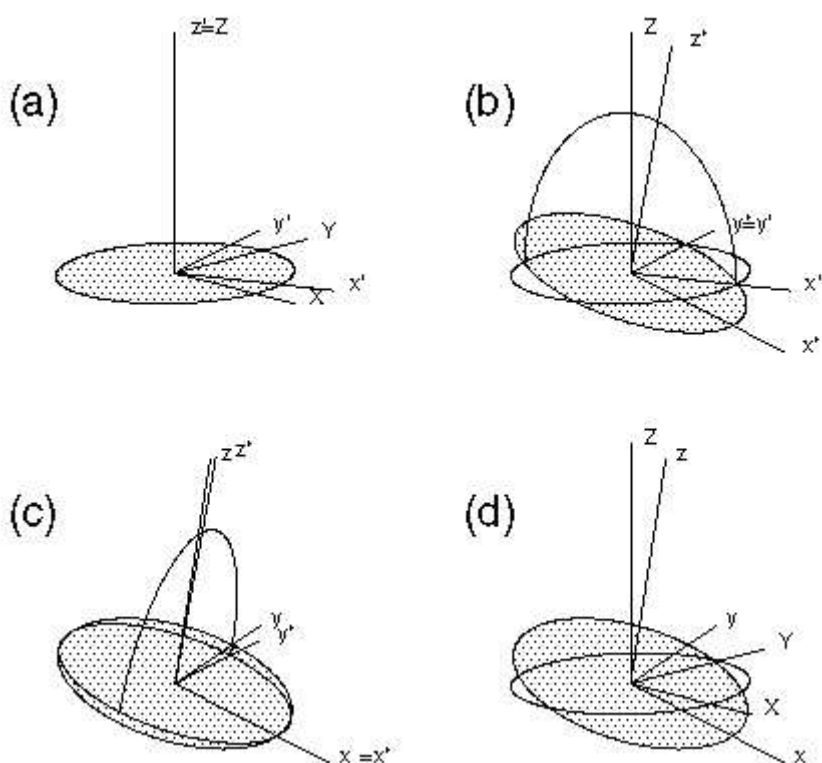


Fig. 4.1.5-I : each panel shows the rotation from the thicker axis system to the thinner one. The first three panels give the individual rotations described above, while the last one gives the overall misalignments. The orientation and rotation relative magnitude corresponds to unit M3, but rotation angles are exaggerated by a factor 100

The relevant coefficients have been calibrated from raster scan observations of a given celestial sources at known pointings. For all practical applications there is no significant rotation (within a couple of degrees) around the Z axis, hence alpha has been fixed to 0° for unit M3 or 180° for unit M1 and M2 (to give the same orientation as the spacecraft axes), while angle beta corresponds to a shift of about 10 arcmin along the x axis for all detectors, and gamma is smaller (between half and 2.5 arcmin) with uncertainties of about a quarter of arcmin.

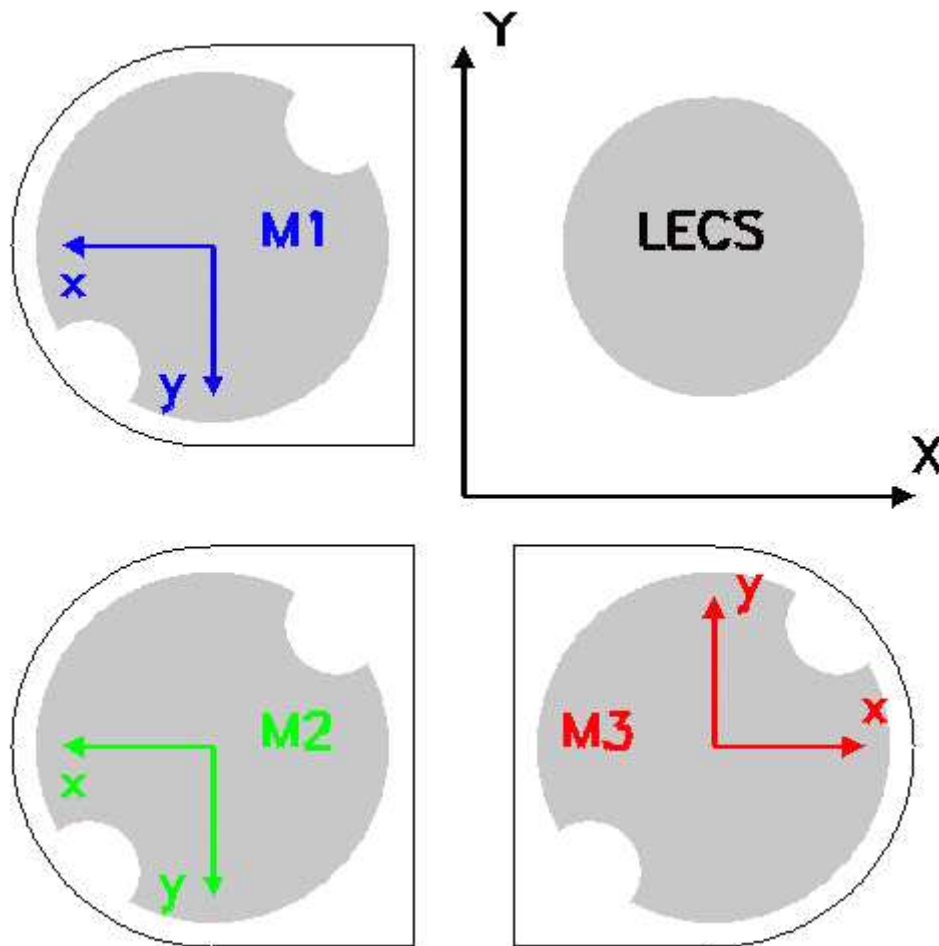


Fig. 4.1.5-II : orientation of MECS units with respect to the spacecraft XY axes

The effect of this is that if the satellite is pointed with its Z axis on the target, the latter will be positioned behind the strongback. This is visible in the [first light pointing](#). The pointing strategy takes account of this, and compensates, placing the source close to the MECS centre, as in the [second light pointing](#).

The coefficients are stored in files `m{1,2,3}.misalignment` and are used by software for [conversion](#) between image and sky coordinates.

4.2 Plasma suppression grid transmission

The transmission of the [plasma suppression grid](#), τ_{g} , is a hardcoded scalar (energy-independent) value of `FILT1=0.921`.

[\[Home\]](#) [\[ToC\]](#) [\[Previous\]](#) [\[Next 4.3 cont.\]](#)

[continues from [4.2](#)]

4.3 Filter transmission

The term τ_{f} is the transmission of the UV and ion [filters](#); it is computed from the atomic parameters of Carbon and Oxygen (for Polycarbon, i.e. Lexan filter) or Carbon, Nitrogen, Oxygen (for Polyamide, i.e. Kapton filter), and Aluminum (both filters) and it is hardcoded in the relevant routines. While for Lexan filter the values supplied by the filter manufacturer are used, for the Kapton filter we show also the measurements by Jager 1996 (private communication).

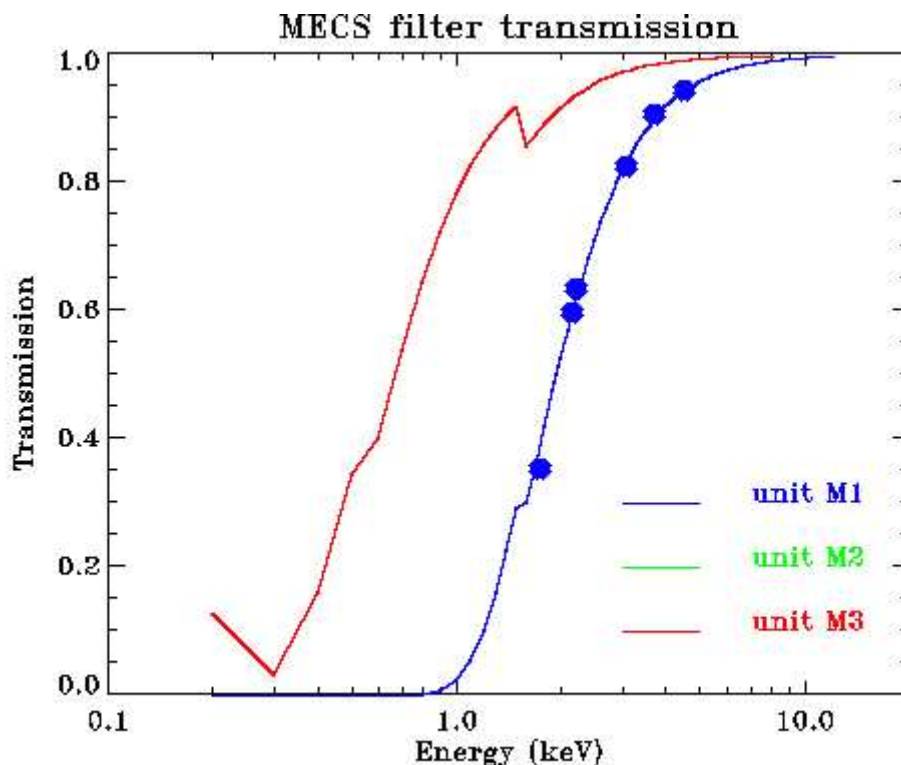


Fig. 4.3-I : MECS filter transmission (NB: M2 and M3 are alike)

The relevant component thicknesses (in mm) are contained in the following files:

- for M1 (Kapton) file [kapton.thickness](#), 10.E-3 mm (Poly-A) and 200.E-6 mm (Al)
- for M2 (Lexan) file [m2_lexan.thickness](#), 0.66E-3 mm (Poly-C) and 95.E-6 mm (Al)
- for M3 (Lexan) file [m3_lexan.thickness](#), 0.66E-3 mm (Poly-C) and 95.E-6 mm (Al)

[\[Home\]](#) [\[ToC\]](#) [\[Previous\]](#) [\[Next 4.4 cont.\]](#)

[continues from [4.3](#)]

4.4 Calibration source parameters

The reference characteristics of the calibration sources are stored in files `m{1,2,3}_calsource.coeff` and are used by the gain history accumulation program. These characteristics are :

- a [reference gain](#)
 - the X and Y coordinates of the two calibration sources in unlinearized coordinates (these are converted in linearized coordinates of user selected pixel size inside the program and are not reported here).
-

4.5 Beryllium window transmission

The term τ_w is the transmission of the Be window at a given energy and position, reported in [fig. 4.5-I](#). Its dependencies are:

- on energy through the Be absorption cross section (computed from atomic coefficients hardcoded in the programs), and
- through the typical thickness of the [window](#) and of the [strongback](#) (currently stored in files `m{1,2,3}_thick_be.dat`), and equal to
 - for M1 : 51.5 micron (window) plus 600 micron (strongback)
 - for M2 : 54.5 micron (window) plus 600 micron (strongback)
 - for M3 : 53.5 micron (window) plus 600 micron (strongback)

- and on position, due to the presence of the strongback structure (this must be convolved with the Point Spread Function of the optics alone)

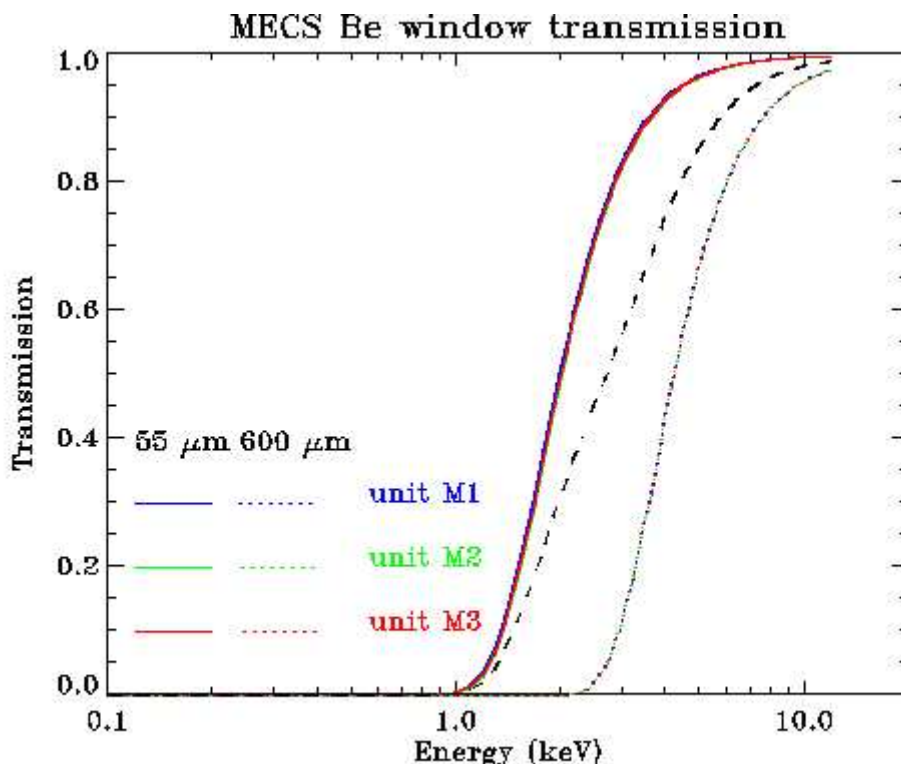


Fig. 4.5-I : Transmission of a Be layer with nominal thicknesses of the MECS entrance window (solid) and its supporting strongback (dotted). The dashed black line is the overall transmission in a point at $x,y = (0,5)$ mm, i.e. on the edge of the strongback.

Namely, the transmission at one given position x,y is computed combining the transparencies of the two thicknesses t_{window} and $t_{strongback}$

$$\tau_w = Z(E,x,y) \exp(-\mu(E)t_{window}) + (1-Z(E,x,y)) \exp(-\mu(E)t_{strongback})$$

where $Z(E,x,y)$ is the convolution of a 1/0 mask representing the Be entrance window with the optics PSF (i.e. the coverage fraction of the window) and its complement $1-Z$ is the coverage fraction of the strongback.

Additional representations (as separately numbered figures) can be obtained via the following form. Please note that the time needed to compute images can be **prohibitively** long (more than 10 minutes) and CPU-intensive : please reserve this option to off-peak hours.

Plot/compute ONE of the following parameters for MECS unit

Item and/or quantity	Symbol	Select
Overall transmission	τ_w	<input checked="" type="radio"/>
Be window layer	τ_{window} or Z_{window}	<input type="radio"/>
strongback	$\tau_{strongback}$ or $Z_{strongback}$	<input type="radio"/>
Be window layer, product	$Z_{window} * \tau_{window}$	<input type="radio"/>
strongback, product	$Z_{strongback} * \tau_{strongback}$	<input type="radio"/>

select ONE type of data representation, the relevant parameter and data format

- transmission τ vs E none
- $v(E)$ at given position x,y mm
- $v(x,y)$ image at E (SLOW!) keV

[\[Home\]](#) [\[ToC\]](#) [\[Previous\]](#) [\[Next 4.6 cont.\]](#)

[continues from [4.5](#)]

4.6 Detector quantum efficiency

The term epsilon is made of two terms corresponding to the two regions of the detector: the drift region where the bulk of the conversion of X-rays into electrons occur, and the scintillation region, where residual conversion of some X-rays may occur.

In both cases the energy dependency is modelled through the Xe absorption cross section (computed from atomic coefficients hardcoded in the programs).

4.6.1 Drift region

The calibration parameters of the drift region in the cell are currently the same for all three MECS units.

The values of these parameters for all three MECS units are stored in file [cell.coeff](#) and are:

- the depth of the drift region : 20. mm
- the Xe density (at 273 °K) : 0.0059 g/cm³

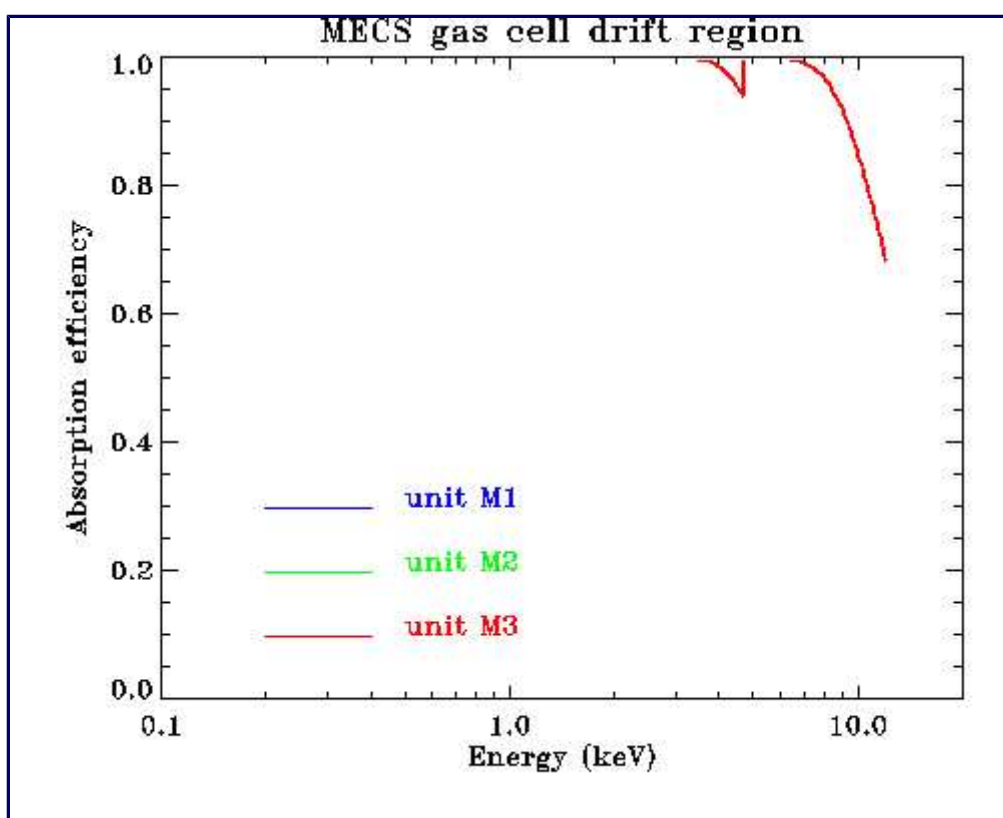


Fig. 4.6.1-I : absorption efficiency in the drift region (click on figure to expand Y scale)

[\[Home\]](#) [\[ToC\]](#) [\[Previous\]](#) [\[Next 4.6.2 cont.\]](#)

[continues from [4.6.1](#)]

4.6.2 Scintillation region

The top fraction of the scintillation region contributes also to the total efficiency; events that interact in this top region produce a BL within the nominal thresholds. This effect can be modelled by a "fudged" layer of Xenon, whose depth is stored in files `m{1,2,3}_scintillation.coeff`

The values are:

- the depth of the M1 active scintillation region : 7.0 mm
- the depth of the M2 active scintillation region : 3.0 mm
- the depth of the M3 active scintillation region : 11.0 mm
- the Xe density (at 273 °K) : 0.0059 g/cm³

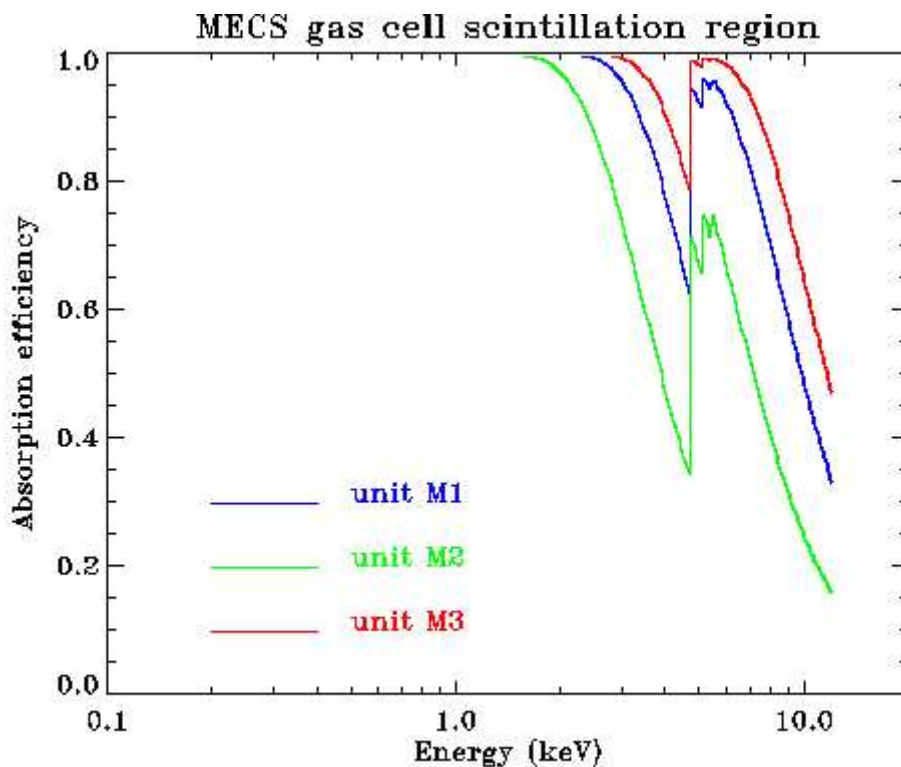


Fig. 4.6.2-I : absorption efficiency in the scintillation region

The overall efficiency of the gas cell is the sum of the [absorption efficiency](#) in the [drift region](#) and of the product of the absorption efficiency in the scintillation region (see [figure above](#)) times the transmission efficiency of the drift region (complement to 1 of the relevant absorption).

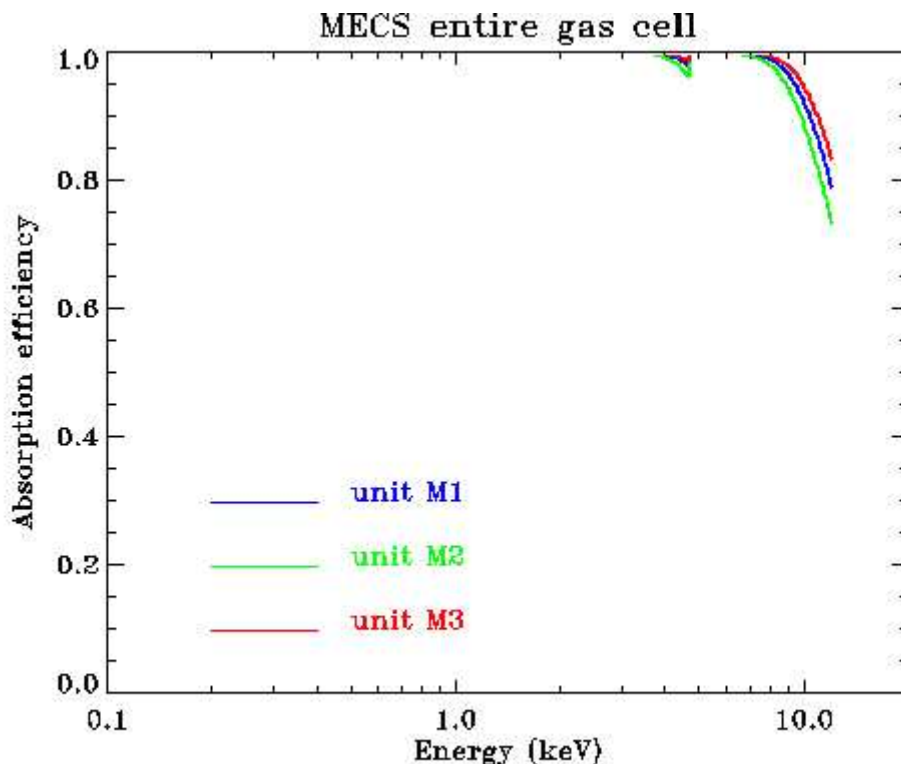


Fig. 4.6.2-II : overall efficiency of the MECS gas cells

[\[Home\]](#) [\[ToC\]](#) [\[Previous\]](#) [\[Next 4.7 cont.\]](#)

[continues from [4.6.2](#)]

4.7 Detector resolution

The detector resolution has been computed from monochromatic line spectra taken at the Panter facility. The typical line has a [Gaussian shape](#) plus a [low energy tail](#).

4.7.1 Gaussian component

The Gaussian component for a given input energy is represented by a gaussian (of arbitrary normalization D_1) centered at the PI channel (D_2) given by the [gain relation](#) broadened with a given sigma (D_3).

$$G_i(E_j) = D_1 \exp(-0.5 [(PI-D_2)/D_3]^2)$$

where PI indicates the i-th output channel.

As customary for proportional counters, instead of the sigma one gives the FWHM as $\Delta E/E$ %. The energy dependency is proportional to $E^{-1/2}$ and therefore a single parameter FWHM6 (the FWHM at 6 keV) is sufficient to describe it:

- for M1 : 8.40 %
- for M2 : 8.04 %
- for M3 : 7.78 %

Such values for the three MECS units are all stored in a single file [resolution.coeff](#).

The sigma at any energy can therefore be easily computed as :

$$\sigma = D_3 = 0.01 \text{ FWHM6 } 6^{1/2} E^{1/2} / 2.355$$

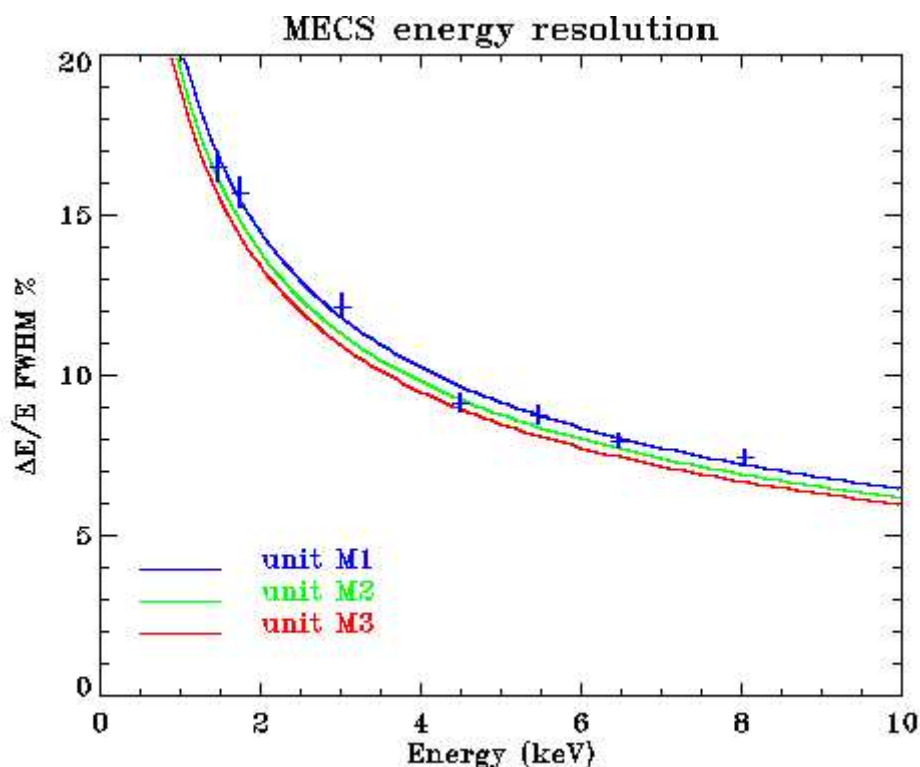


Fig. 4.7.1-I : MECS spectral resolution
We report also, as example, experimental measurements for M1.

[\[Home\]](#) [\[ToC\]](#) [\[Previous\]](#) [\[Next 4.7.2 cont.\]](#)

[continues from [4.7.1](#)]

4.7.2 Low energy tail

A monochromatic line gives rise not only to a Gaussian line, but shows also a tail on the low energy side (extending below 1 keV where the [Be window](#) is not transparent). The physical reason is that part of the electrons generated by an X-ray may attach to the Be window itself instead of propagating in the drift region (see [GSPC operation](#)).

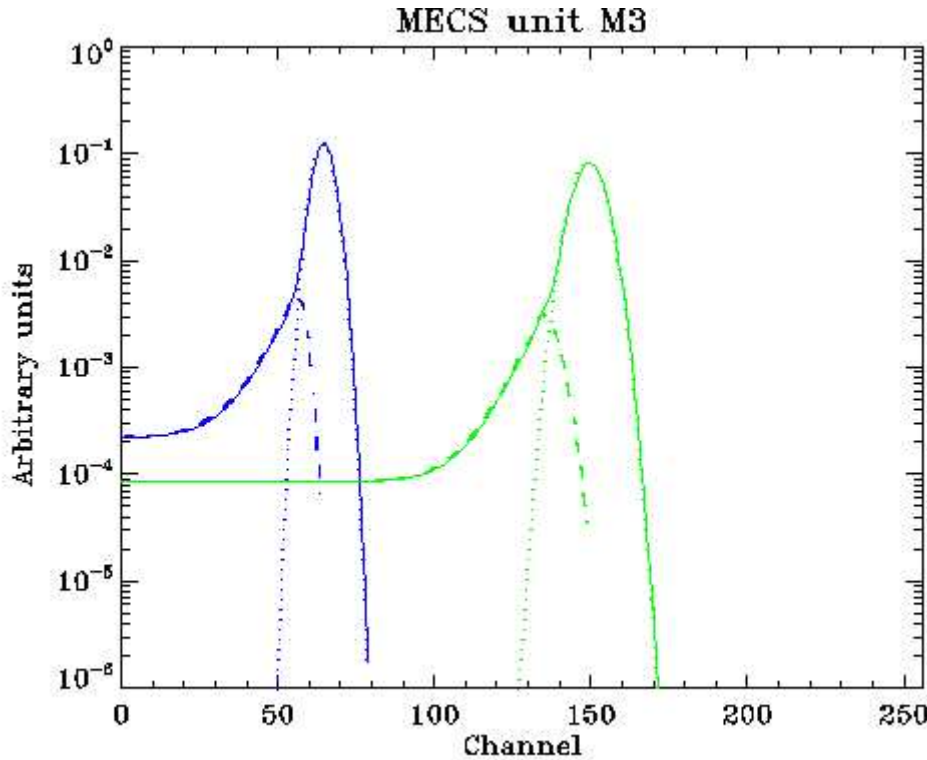


Fig. 4.7.2-I : Example of the spread of a simulated spectrum generated by a 3 keV and 7 keV monochromatic line. The gaussian and tail components (unnormalized) are shown, as well as their (normalized) combination.

The tail is empirically modelled by a complex function (defined only above 1.255 keV) :

$$T_i(E_j) = D_4 + D_5 \exp\left(\frac{PI - D_6}{D_7}\right) \quad \text{if } PI < D_6$$

$$T_i(E_j) = D_5 \exp\left(-0.5 \left[\frac{3(PI - D_6)}{D_2 - D_6}\right]^2\right) \quad \text{otherwise}$$

where the symbols are as follows :

- PI indicates the i-th output channel
- D_2 is the peak of the [gaussian component](#) of given energy, given by the [gain relation](#)
- D_4 is computed indirectly as a function of energy as a quadratic polynomial of the Xenon absorption efficiency (3 coefficients $L_{1,1}$, $L_{1,2}$, $L_{1,3}$ necessary)
- D_5 depends on other terms and is given by formula

$$D_5 = (C/D_7) / (1 - \exp[(L_4 - D_6)/D_7])$$

- where C is a quadratic polynomial of energy up to 8.04 keV, then remains constant (3 coefficients $L_{2,1}$, $L_{2,2}$, $L_{2,3}$ necessary)
- D_6 is given by a linear function of energy in two separate stretches (of same slope $L_{5,3}$, but with two different intercepts $L_{5,1}$ and $L_{5,2}$ below and above the Xenon L-edge)
- D_7 is computed via the gain relation from a single coefficient L_3
- L_4 is an independent coefficient giving the start channel above which the tail is defined

The values of the coefficients L are kept in files `m{1,2,3}_tail.coeff`
The notation $L_{i,j}$ refers to the i-th line and j-th position in line in the file.

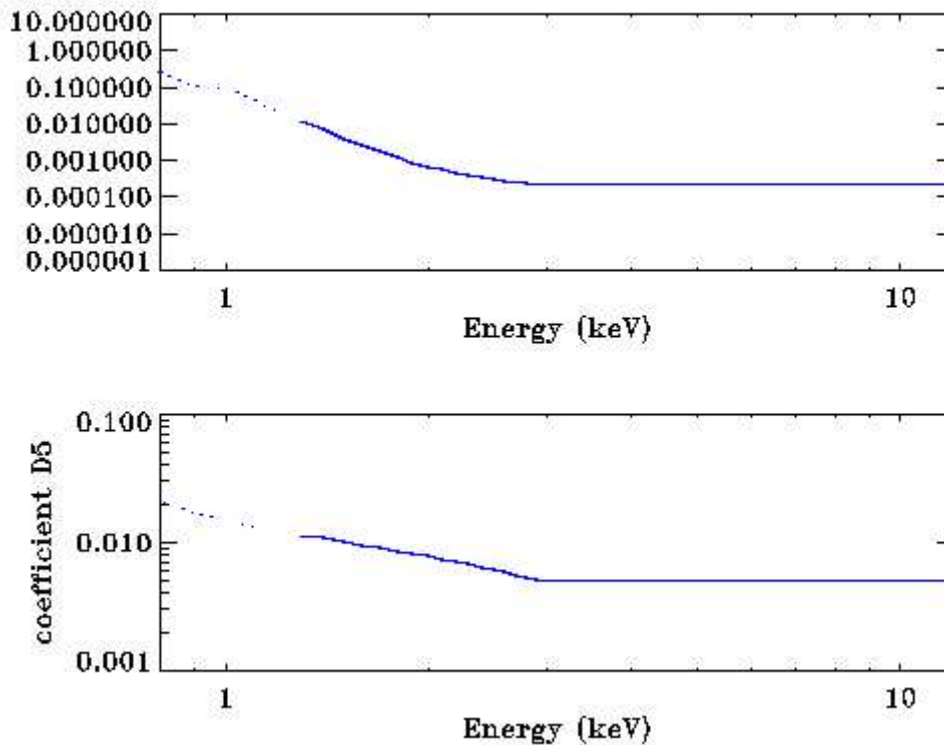


Fig. 4.7.2-II : Energy dependency of tail parameters D_4 and D_5 . The values for the different MECS units (colours) are quite similar. Note that coefficients are meaningless (dotted line) below 1.25 keV where the tail is not defined.

Additional representations of simulated spectra can be obtained via the following form. Data is always generated for the three MECS units.

Select energy keV, representation and type of spectral component

Gaussian component (unnormalized)

Tail component (unnormalized)

Their combination (normalized)

[\[Home\]](#) [\[ToC\]](#) [\[Previous\]](#) [\[Next 4.8 cont.\]](#)

[continues from [4.7.2](#)]

4.8 Escape fractions

X-rays at energies harder than the Xe-L edge (4.78 keV) have a finite probability of giving rise to a fluorescence photon. This [fluorescence photon](#) may recombine (in this case a photon at its proper energy E is detected, although the Burst Length may be anomalous) or escape from the Be window (in this case a photon is detected at the residual energy).

The escape probability (escape fraction) depends on the geometry of the cell and on the gas filling pressure.

The effect is the presence of line-type features in the low energy spectrum (a line at E will give rise to a secondary peak at $E - E_{\text{fluor}}$). The effect is complicated by the fact that the Xe L-edge has a fine structure (see [simulated spectra](#)). In the case of the MECS, four main escape peaks are detected; their description is given by:

$$EF_f(E_j) = H1_f + H2_f \exp(-0.5 [(E_f - 4.782)/H3_f]^2)$$

where E_{fluor} is the energy of the considered fluorescence photon.

The relevant coefficients (in the order E_{fluor} , H2,H3,H1) are kept in files `m{1,2,3}_escape.coeff`

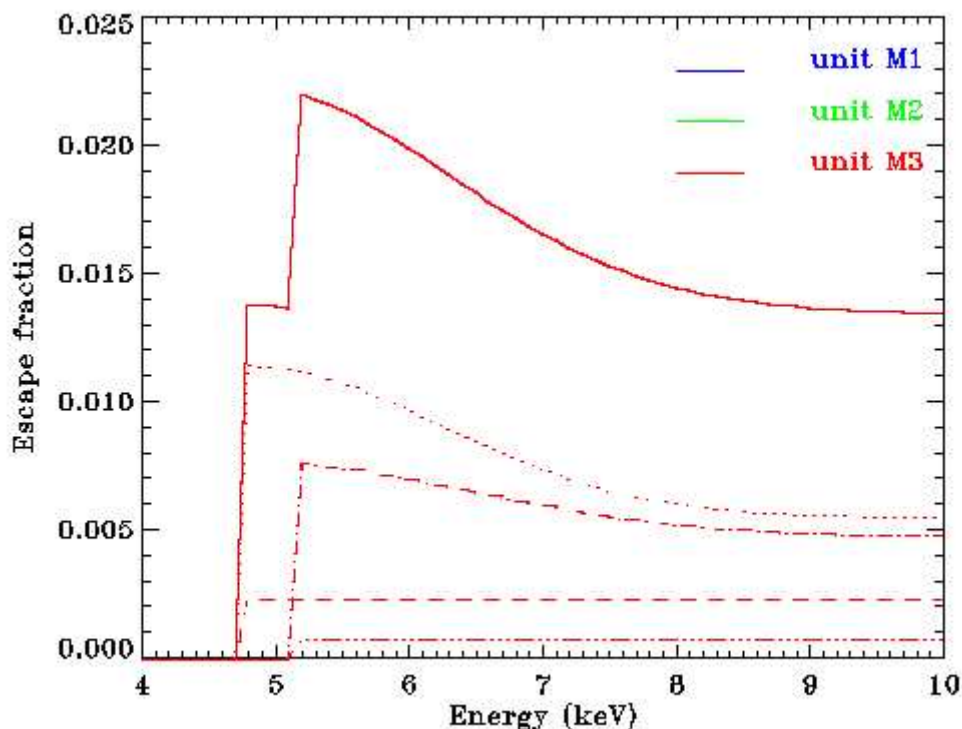


Fig. 4.8-I : MECS escape fraction as function of energy.

Dotted/dashed lines indicate the four components, and the solid line the total escape fraction. Note that currently the same coefficients are used for the 3 MECS units

Additional representations of simulated spectra showing the escape peaks can be obtained via the following form.

Select energy keV, representation and MECS unit

[\[Home\]](#) [\[ToC\]](#) [\[Previous\]](#) [\[Next 4.9 cont.\]](#)

[continues from [4.8](#)]

4.9 Linearization coefficients

The position of a photon is computed by the [Electronics Unit](#) based on the output of the [PMT](#). This process introduces a geometrical distortion because of three effects :

- spatial disuniformity of the PMT [gain](#) (energy independent)
- different viewing angles of different scintillation positions (energy independent)
- curvature of the [Be window](#) with associated distortion of the electric field (energy dependent), due to the difference of pressure between the inside of the gas cell and the vacuum outside.

The relevant distortion has been modelled using ground measurements with a [multipinhole mask](#), and it is given as a third-order polynomial relation converting unlinearized x,y pixel positions into linearized X,Y positions in mm:

$$X = A_3(1+A_5/E) (x-A_1) + A_7 (x-A_1)^2 + A_9 (x-A_1)^3$$

$$Y = A_4(1+A_6/E) (y-A_2) + A_8 (y-A_2)^2 + A_{10} (y-A_2)^3$$

In practice the above formula corresponds to a stepwise procedure in which :

- the coordinates are referred to the detector centre (A_1, A_2)
 $x' = x - A_1$

$$y' = y - A_2$$

- the distortion is described by a third-order polynomial in x', y'
- the energy dependency is in the first-order terms only
- in the software a further step is added converting back from X,Y positions in mm to pixels of user-selected (arbitrary) size X', Y'
- in addition the software randomizes the original x, y position within plus or minus half a pixel, in order to prevent artifacts due to integer-to-real conversion

The ten coefficients A_1 to A_{10} are kept in files `m{1,2,3}_xy.coeff`

[\[Home\]](#) [\[ToC\]](#) [\[Previous\]](#) [\[Next 4.10 cont.\]](#)

[continues from [4.9](#)]

4.10 MECS gain

The term gain customarily refers to the relationship linking PHA or PI channels and energy. In the case of the MECS we ultimately deal with PI channels. The gain relation is not uniform all over the surface of the detector, and is sensitive to temperature variation. It also depends on the High Voltage setting (particular the one of the PMT). All these effects may be compensated, and one can refer the gain to the detector centre at a standard gain.

4.10.1 Gain coefficients

The relation between PI channels and energy is described by the following stepwise formula with four linear and parallel stretches (currently all G_i coefficients are equal for a given unit)

$$\begin{aligned} PI &= G_1 E + O_1 && (E < E_1 = 4.78 \text{ keV}) \\ PI &= G_2 E + O_2 && (4.78 < E < E_2 = 5.10 \text{ keV}) \\ PI &= G_3 E + O_3 && (5.10 < E < E_3 = 5.44 \text{ keV}) \\ PI &= G_4 E + O_4 && (E > 5.44 \text{ keV}) \end{aligned}$$

where the jumps occur in correspondence of the structure of the Xe L-edge.

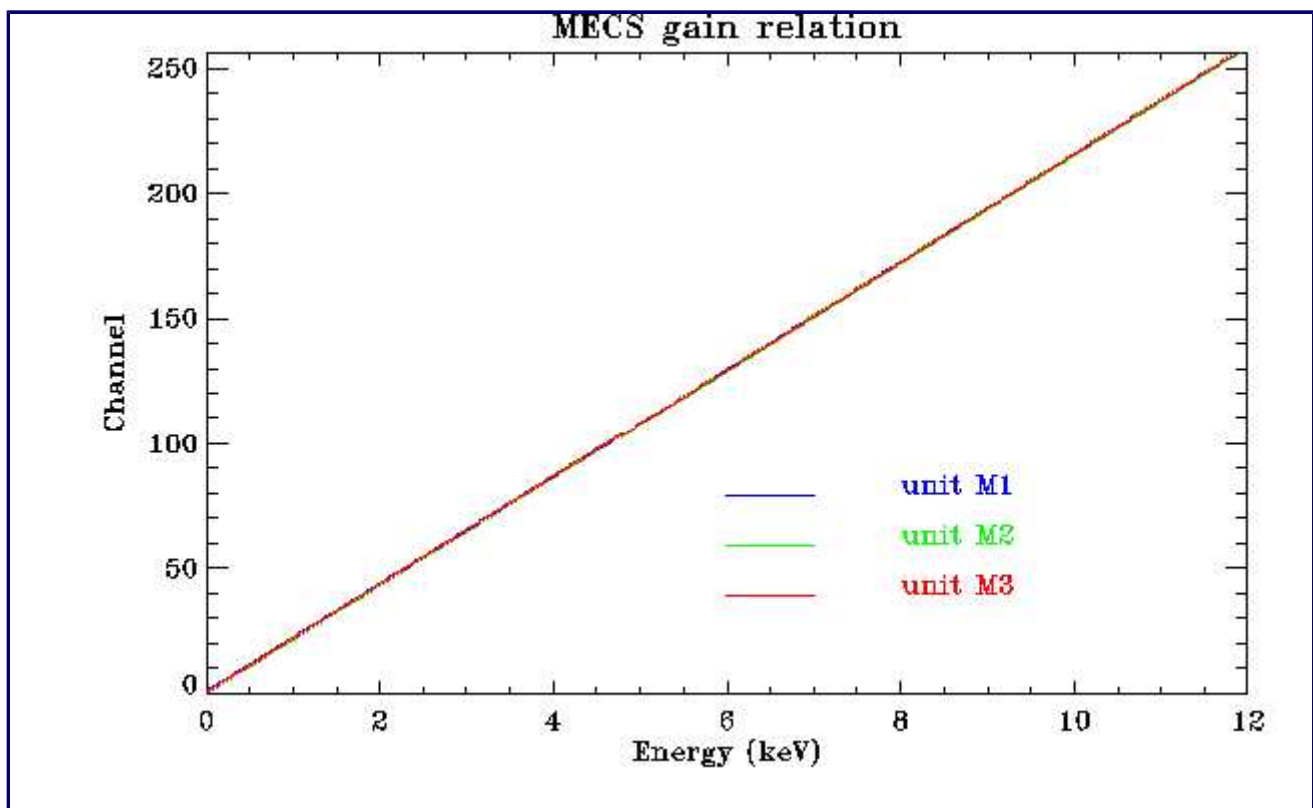


Fig. 4.10-I : MECS gain relation (click on picture to enlarge)

The relevant coefficients (in order, the E_i , G_i and O_i) are kept in files `m{1,2,3}_gain.coeff`

Note that one has to **add 1** to the above PI numbers if one wishes to number channels from 1 to 256 (this is done in the matrix routines and in the figure above), while one uses the original coefficients to match the telemetry numbering (0-255), like in the [gain correction](#) routines

Each MECS unit has its own energy-channel relation; however, for uniformity purposes and to improve signal to noise at some expense of energy resolution, someone uses to equalize them to the M1 unit relation.

[\[Home\]](#) [\[ToC\]](#) [\[Previous\]](#) [\[Next 4.10.2 cont.\]](#)

[continues from [4.10.1](#)]

4.10.2 Positional dependency

The gain of the detector is not uniform across the detector surface. This dependency is essentially due to disuniformities in the [PMT](#) and is strictly independent of energy.

Maps of the relative gain vs unlinearized position have been determined on the ground measuring the position of reference lines at different positions using a [multipinhole mask](#). Since there is no dependency on energy, all maps have been averaged, allowing to determine the relative gain with an uncertainty of 0.3 % in the central part of the field of view (the uncertainty is higher close to the calibration sources, because of lack of close multipinhole measurements).

The relative gain maps are kept in XAS image form in (binary) files `m{1,2,3}_gain.image`. Access and display of such data (as separately numbered figures) is possible via the following form:

Unit :	<input type="text" value="M1"/>
Data :	<input type="text" value="Relative Gain"/>
Output :	<input type="text" value="GIF image file"/>
<input type="button" value="Proceed"/>	

[\[Home\]](#) [\[ToC\]](#) [\[Previous\]](#) [\[Next 4.10.3 cont.\]](#)

[continues from [4.10.2](#)]

4.10.3 Time (Temperature) dependency

The temperature dependency is fully compensated monitoring the gain of the [built-in calibration sources](#) and generating a [gain history](#).

Therefore there are no associated additional calibration files.

The following example shows the typical time dependency of the relative gain. It also shows a [temperature HK](#) parameter available to observers (PMT power supply temperature). There is a clear (anti-)correlation with the overall temperature trend (envelope of the temperature profile), i.e. the increase of environment temperature after the first switch on, and the diurnal modulation. There is (fortunately) no correlation with short-term temperature variations due to on-off orbital cycling.

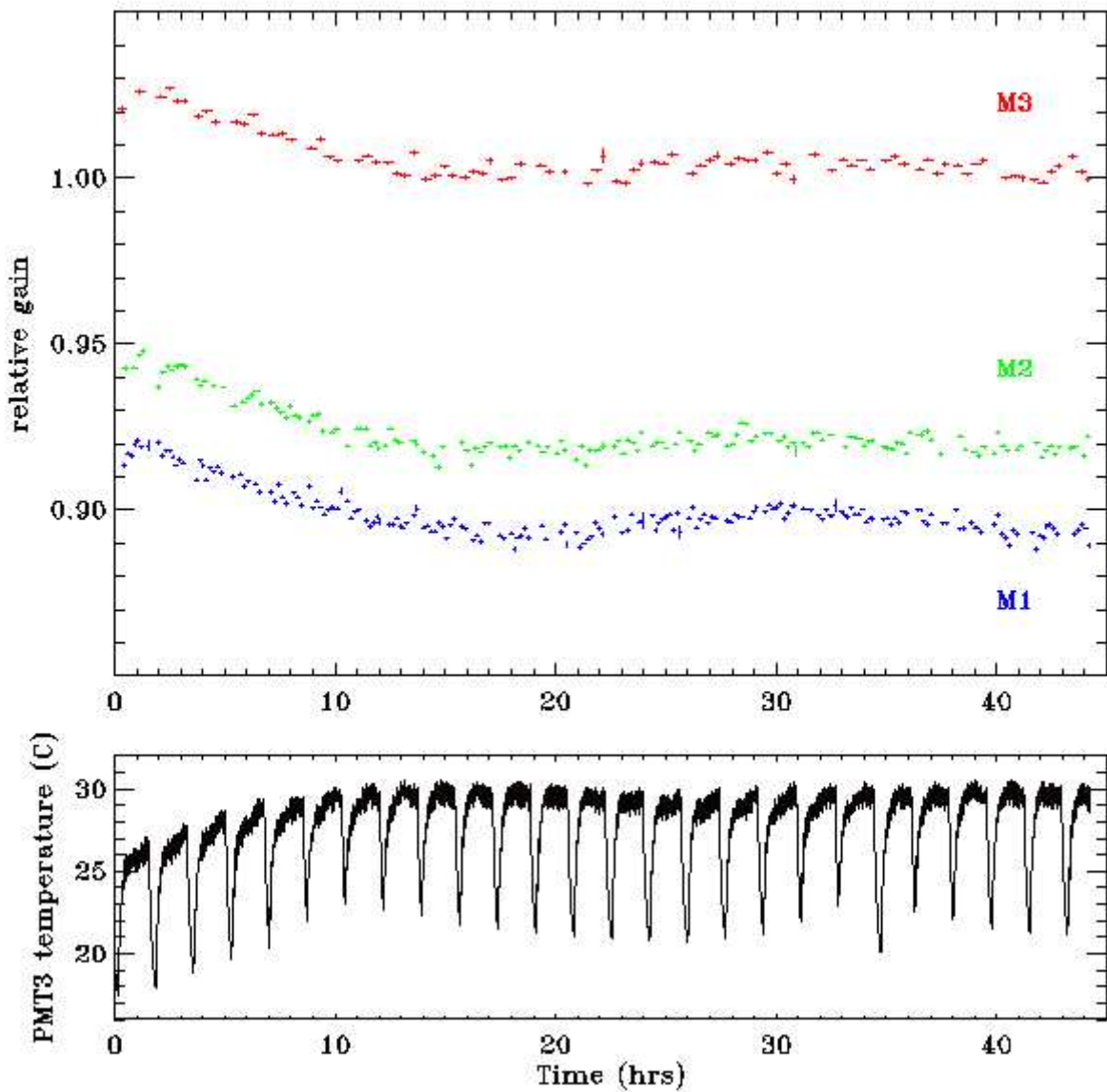


Fig. 4.10.3-I : Example of gain history

The spectra of the calibration sources (referred to detector centre), corresponding to the first and last point of the above M1 gain history, are reported below.

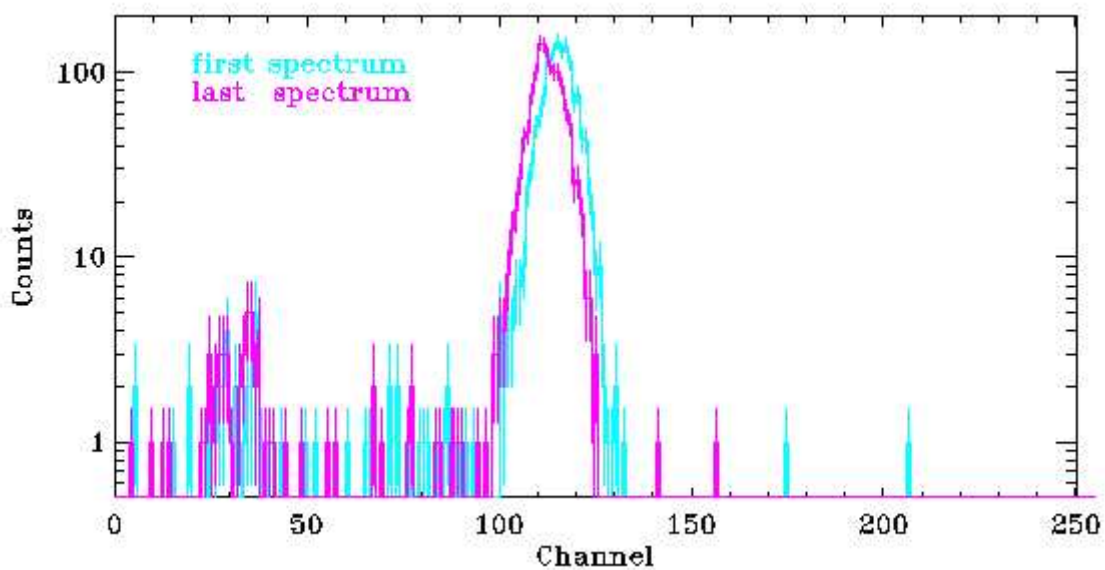


Fig. 4.10.3-II : Example of calibration source spectra, showing typical gain variation

A more precise correlation exists with a different [temperature HK](#) parameter, which however is transmitted in the spacecraft (TCU) telemetry, and is not normally available, the DU box temperature (which is not influenced by short term power cycling). SVP observations allowed to verify the existence of a linear trend of gain with temperature.

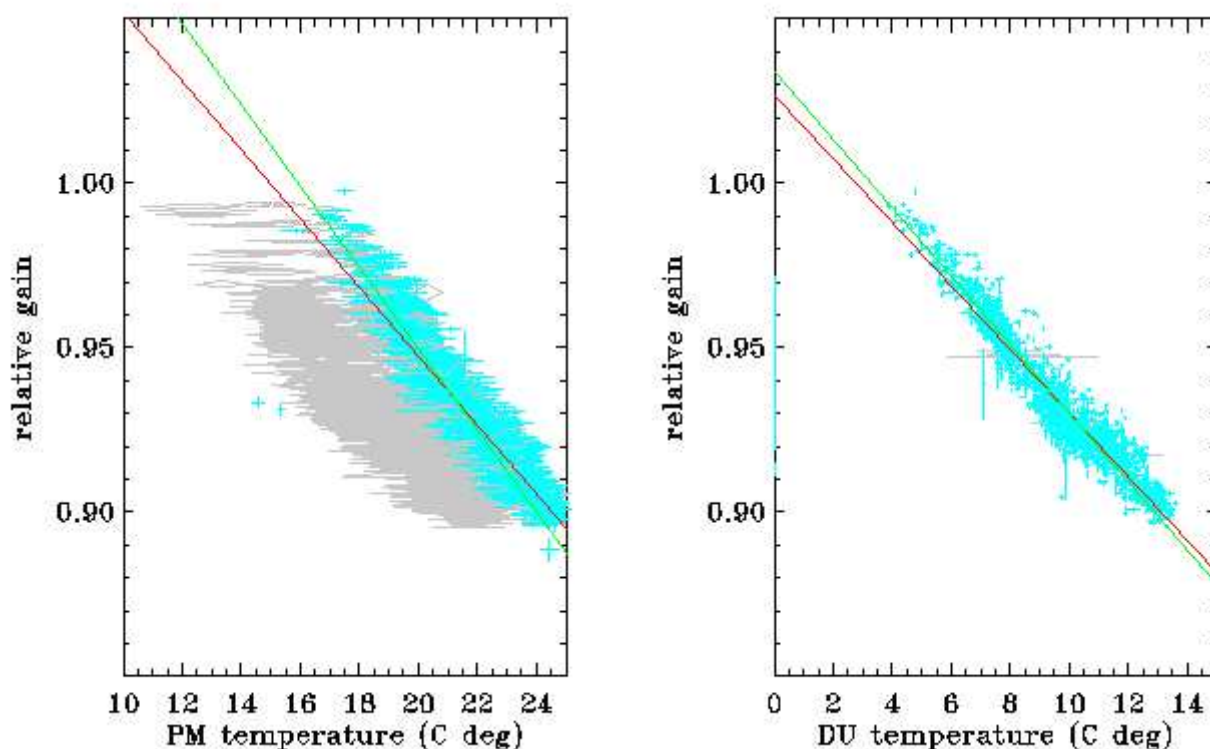


Fig. 4.10.3-III : Example of gain-temperature correlation (unit M1), covering almost all Performance Verification phase.

Left frame is for PMT temperature, right frame for DU box temperature. For the PMT case, good temperature values (when instrument is stably on) are in cyan, while gray indicates unstable temperature during switch on.

These are the typical coefficients of the correlation (derived from a "direct" linear fit of gain vs T, and also from a "reverse" fit of T vs gain, indicated in different colours in figure above).

unit	gain vs PMT temperature		gain vs DU temperature	
	direct	reverse	direct	reverse
M1	$g=1.155-0.0104T$	$g=1.196-0.0123T$	$g=1.027-0.00965T$	$g=1.034-0.0104T$
M2	$g=1.110-0.0079T$	$g=1.186-0.0117T$	$g=1.050-0.00886T$	$g=1.066-0.0104T$
M3	$g=1.197-0.0066T$	$g=1.224-0.0076T$	$g=1.088-0.00573T$	$g=1.097-0.0063T$

4.10.4 Absolute reference

The reference gain to which all gains are normalized is contained in the [calibration source](#) characteristics file: the normalization is such that channel 125.5 corresponds to the energy of the ^{55}Fe calibration line (5.894 keV) for all three MECS units, which is only a rough equalization.

4.10.5 The channel boundaries

The photon energy is reported in the telemetry as a raw PHA value (range 0-255). These values are usually [corrected](#) during the accumulation for all gain effects and are therefore normalized to a standard scale (sometimes called "PI" or "Pulse Invariant" channels).

The boundaries of the channel in a spectrum have no particular physical meaning and do not enter the convolution procedure, but are used just to plot spectra on an energy scale. They are conventionally produced using the [gain relation](#) with an offset O_* being the average between O_1 and O_4 .

[\[Home\]](#) [\[ToC\]](#) [\[Previous\]](#) [\[Next 4.11 cont.\]](#)

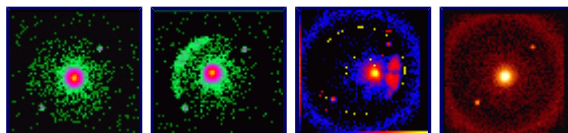
[continues from [4.10.5](#)]

4.11 The Point Spread Function

The Point Spread Function of an entire MECS unit ([Mirror Unit](#) and [Detector Unit](#)) has been carefully calibrated on the ground [1,4] and verified in flight [2]. Its on-axis shape is remarkably well described by a radial distribution which applies also well within 6 (or may be 10) arcmin from the centre.

Some examples of monochromatic PSF taken on the ground are reported separately for [on-axis](#) and [off-axis](#) cases. The off-axis PSF shows a gradual deviation from a radial distribution, with an elongation of the core in the tangential direction, and the appearance of the effect of single reflections in the wings. Note that all scales are logarithmic.

See also the Cyg X-1 [first light](#) (off-axis, behind the [strongback](#)) and [second light](#) (on-axis) taken in flight during the [commissioning phase](#).



The on-axis differential PSF can be modelled analytically as the sum of a Gaussian and a generalized Lorentzian component, whose coefficients depend on energy.

$$G(r) = c_g \exp [-0.5(r/\sigma)^2] = c_g G_s(r)$$

$$L(r) = c_l [1+(r/r_l)^2]^{-m} = c_l L_s(r)$$

An example of the differential PSF shape is shown here below (additional figures can be [produced in a customized way](#)).

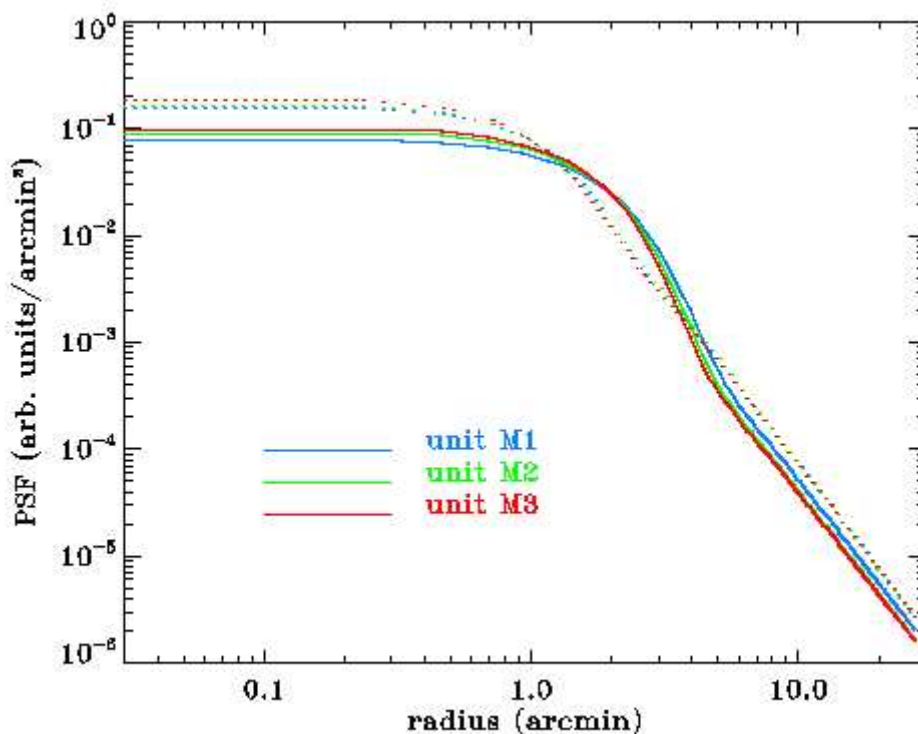


Fig. 4.11-I : MECS differential PSF (analytical form) at 2 (solid) and 8 keV (dotted)

The normalization of the integral of the PSF over the entire plane to 1 allows to remove one free parameter, and use just $R = c_g/c_l$ to reduce the expression to the following, taking advantage of the "simplified" forms of the Gaussian and Lorentzian G_s and L_s :

$$PSF(r) = N^{-1} \{ R G_s(r) + L_s(r) \} \quad \text{i.e.}$$

$$PSF(r) = N^{-1} \{ R \exp[-0.5(r/\sigma)^2] + [1+(r/r_l)^2]^{-m} \} \quad \text{with}$$

$$N = 2\pi [R \sigma^2 + r_l^2 / 2(m-1)]$$

where the parameters R , r_l , σ and m depends on energy. Such dependency has been modelled empirically for each parameter using a function of the form :

$$parameter = d + eE + c \exp[-(E-a)/b]$$

where there is a different set of coefficients a, b, c, d, e for each parameter, and in addition the parameters with dimension of a length (r_l and σ) may be subject to a further scale factor, according to whether r is measured in mm or arcmin.

These coefficients are stored in files used for, and described with, the calculation of the [integral PSF correction factor](#), while their energy dependency is shown here.

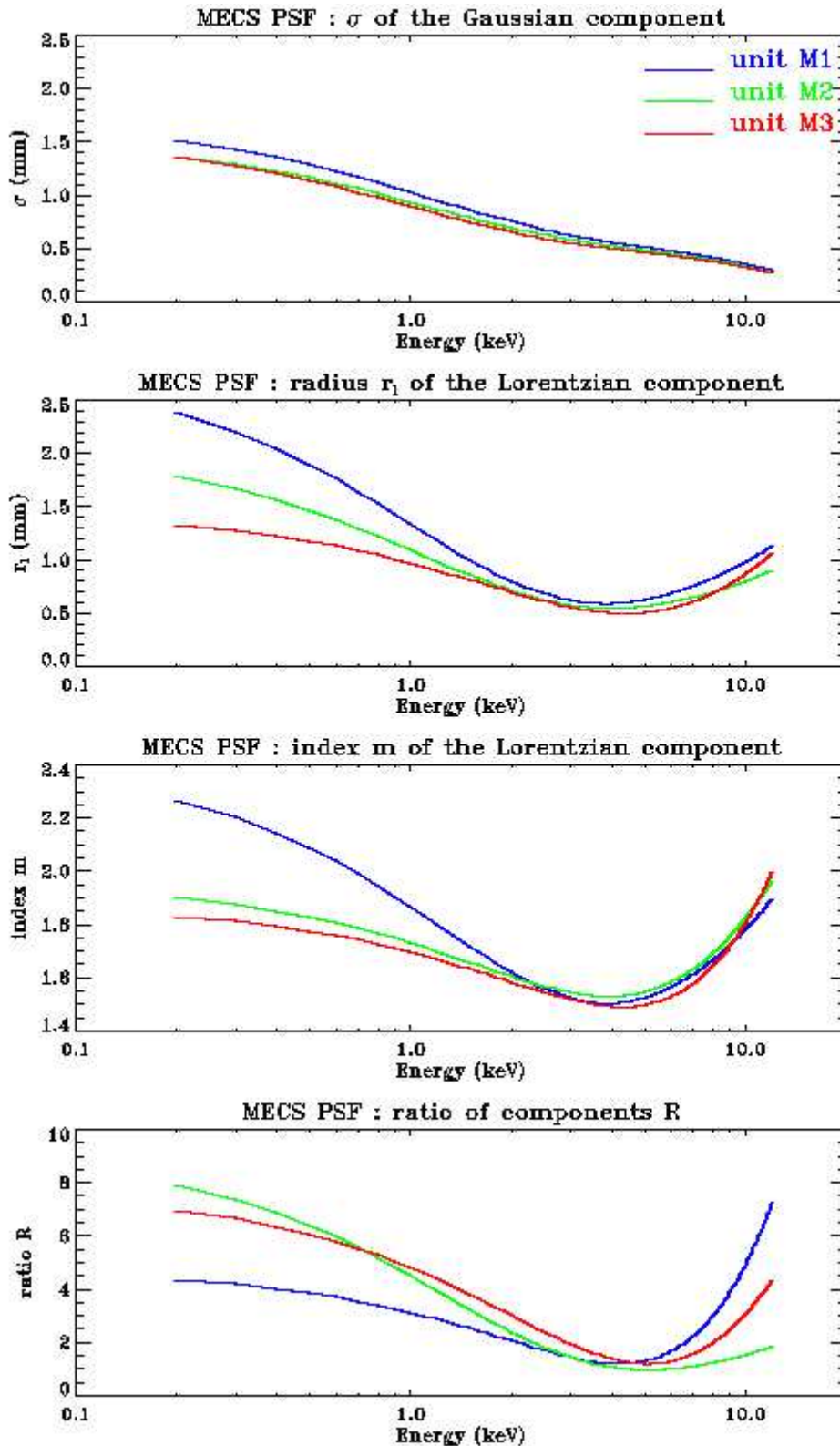


Fig. 4.11.II : Energy dependency of the MECS PSF parameters

Additional representations of (analytically-generated) differential PSF's can be obtained via the following form.

Select energy keV, representation and MECS unit

[\[Home\]](#) [\[ToC\]](#) [\[Previous\]](#) [\[Next 4.11.1 cont.\]](#)

[continues from [4.11](#)]

4.11.1 The PSF of the Mirror Units

The PSF of the optics alone was also calibrated on the ground [\[4\]](#) and is well described as a sum of four Lorentzians ($i=1,4$) of the form :

$$L_i(r) = G_i(E) / \{ \pi B_i(E)^2 [1 + (r/B_i(E))^2]^2 \}$$

The relevant coefficients G_i and B_i depend on energy (via a rough linear interpolation), are the same for all MECS units, and are kept (expressed for r in mm) in calibration file [psf_mir.dat](#).

The coefficients are used **exclusively** to compute the [transmission of the Be window as a function of position](#), since the [strongback](#) is illuminated by a beam broadened by the optics PSF only. Please do not be misled, for any other purpose the [optics+detector PSF](#) is used.

Additional figures can be produced using the following form :

kind of representation	parameter form
<input type="radio"/> B and G coefficients vs energy	none <input type="text" value="Plot"/>
<input checked="" type="radio"/> Differential PSF(E,r) vs r at fixed energy E	<input type="text" value="5.0"/> keV <input type="text" value="Plot"/>
<input type="radio"/> Integral PSF(E,r) vs r at fixed energy E (aka Encircled Energy Function)	<input type="text" value="5.0"/> keV <input type="text" value="Plot"/>

4.11.2 The PSF of Detector

The PSF of the detector alone has a gaussian shape and can be measured on the ground without the optics, either directly using pin-holes, or indirectly using [flat field](#) illumination (e.g. from the shape of the detector window borders). However since it does not enter directly any flight relevant parameter, there are no calibration files associated with it.

[\[Home\]](#) [\[ToC\]](#) [\[Previous\]](#) [\[Next 4.11.3 cont.\]](#)

[continues from [4.11.2](#)]

4.11.3 PSF correction factor

The factor $f(E,r)$ which enters in the response matrix calculation is the fraction of counts falling in a circle of radius r mm, i.e. the integral of the [radial PSF](#) between 0 and r . More precisely one computes the Integral PSF as :

$$IPSF(q) = 2 \pi * \text{integral between 0 and } q \text{ of } PSF(r) r dr$$

taking advantage of the fact that the Gaussian and Lorentzian components entering the definition of [PSF\(r\)](#) can be integrated analytically in $r dr$.

The resulting formula (where the fraction f is normalized to the detector radius r_{det} (FOV radius) of 15 mm) is of the form

$$f(E, r) = IPSF(r) / IPSF(r_{det})$$

$$IPSF(r) = IG(r) + IL(r)$$

$$IG(r) = R \sigma^2 (1 - \exp[-0.5(r/\sigma)^2])$$

$$IL(r) = r_{\perp} \{1 - 1 / [1 + (r/r_{\perp})^2]^{m-1}\} / 2(m-1)$$

and depends on the same four parameters R , r_{\perp} , σ and m already described for the differential [PSF\(r\)](#). As already explained, each one of them in turn depends on energy via [five coefficients](#)

The relevant coefficients are kept in files $m\{1, 2, 3\}_{psf}.coeff$ while [their energy dependency](#) is shown elsewhere.

We report here some examples of the PSF correction factor (normalized integral PSF).

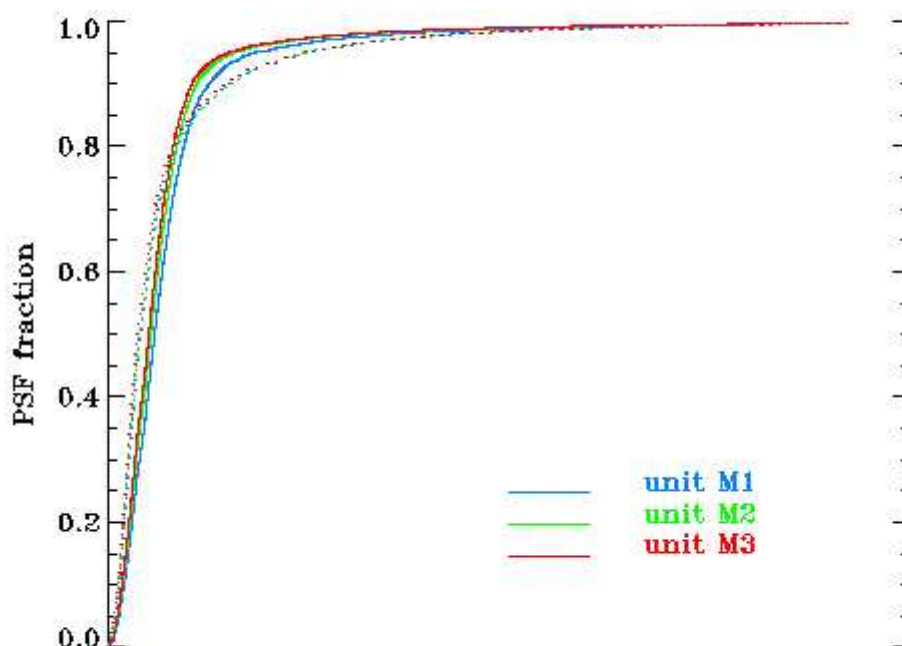


Fig. 4.11.3-I : MECS integral PSF (analytical form) at 2 (solid) and 8 keV (dotted)

while additional representations of (analytically-generated) integral PSF's can be obtained via the following form.

Select MECS unit then after having filled the following form

kind of representation	parameter	form
<input checked="" type="radio"/> f(E,r) vs r at fixed energy E	<input type="text" value="5.0"/> keV	<input type="text" value="Plot"/>
<input type="radio"/> f(E,r) vs E at fixed extraction radius	<input type="text" value="5.0"/> mm	<input type="text" value="Plot"/>
<input type="radio"/> f(E,r) vs E at fixed extraction radius	<input type="text" value="9.3"/> arcmin	<input type="text" value="Plot"/>

[\[Home\]](#) [\[ToC\]](#) [\[Previous\]](#) [\[Next 4.12 cont.\]](#)

[continues from [4.11.3](#)]

4.12 Burst Length corrections

A first correction for BL selection to the total efficiency is taken into account in modelling the scintillation region. A further term has to be introduced to consider the loss of efficiency due to the

high BL threshold. The factor $b(E, B_1, B_2)$ which enters in the response matrix calculation is a correction factor to the efficiency which depends on the Burst Length limits B_1 and B_2 used during the accumulation. This is **currently** modelled by a function only for one fixed optimal range B_1, B_2 : such range (27-60 for M1 and M3, 25-55 for M2) is the one which **must** be used when generating the response matrix.

$$b(E, B_1, B_2) = 1 \quad \text{if } E < F_1$$

$$b(E, B_1, B_2) = F_2 + F_3 \exp[(E - F_1)/F_4] \quad \text{otherwise}$$

The relevant coefficients F (together with B_1 and B_2) are kept in files `m{1,2,3}_blsel.coeff`.

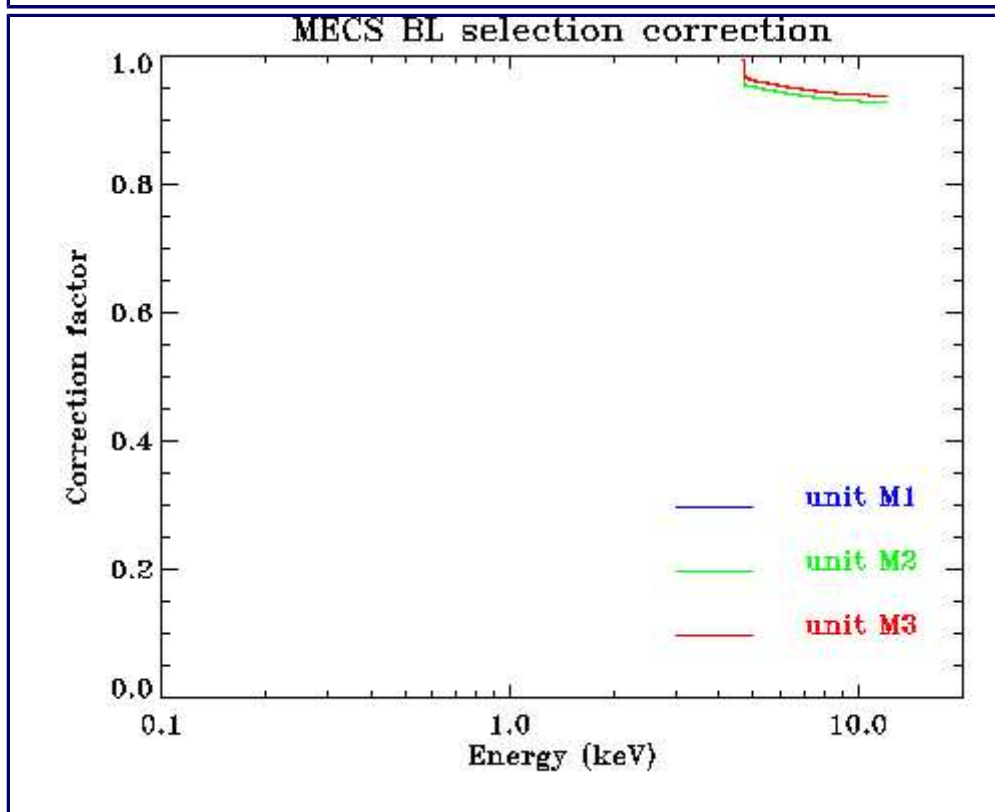
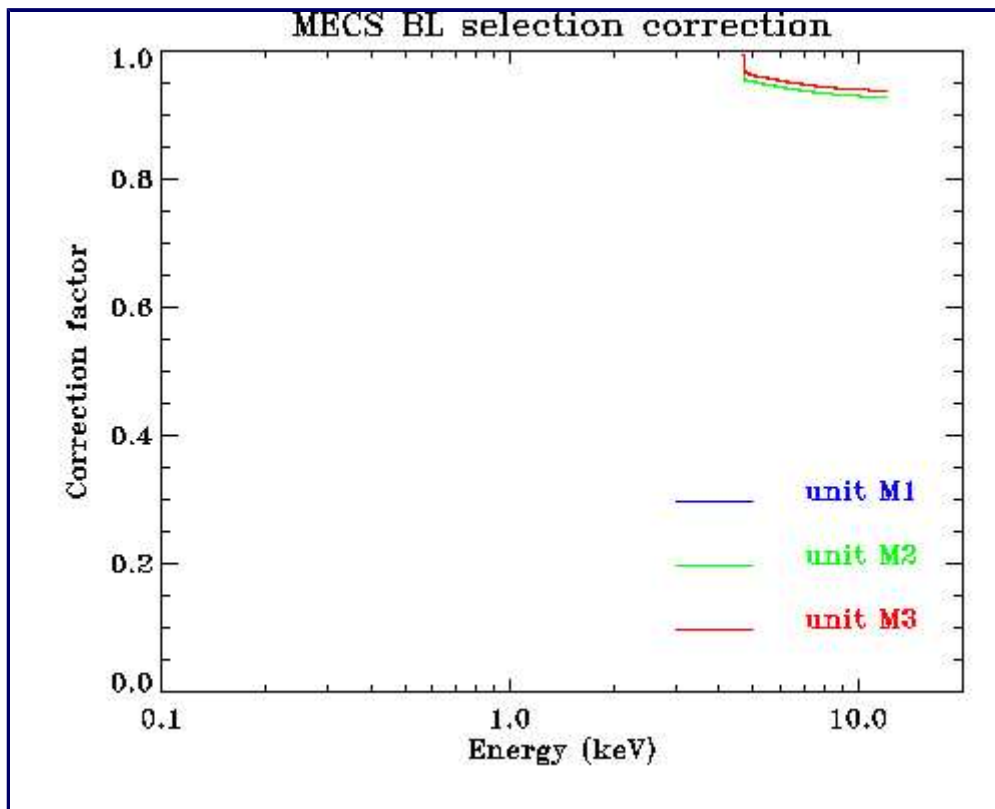


Fig. 4.12-I : MECS BL selection coefficients vs energy (click on figure to expand Y scale)

The following figure shows a typical energy-burst length image (number of counts vs PHA channel on X-axis, and BL channels on Y-axis, both ranging 0-255).

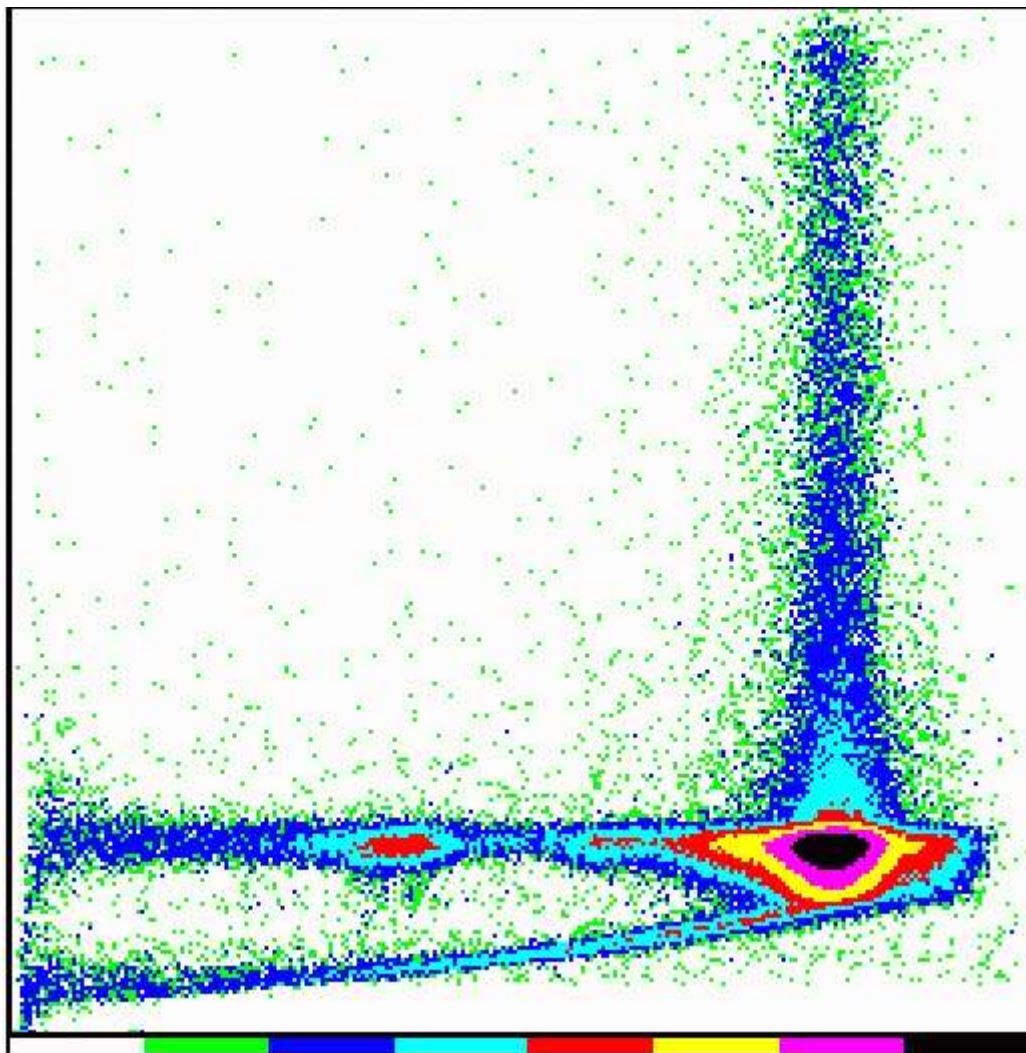


Fig. 4.12-II : example of E-BL image for an exposure taken on the ground (MPE Panter facility) This particular exposure is in Cu light (8.4 keV). The X and Y scale are in PHA and BL channels (both ranging 0-255).

The horizontal strip corresponds to the normal BL range, and contains the continuum underlying the line, the line itself (i.e. the events numbered as 1-2 in the [event interaction figure](#)), and the [escape peak](#) (fluorescence events numbered as 4). The vertical strip is due to events indicated with number 3 (recombination of primary and fluorescence at long BL). The lower oblique branch is due to events (not shown in quoted figure) absorbed in the scintillation region with a lower penetration depth (they produce a reduced amount of UV light, resulting in a shorter BL and a wrong PHA value).

[\[Home\]](#) [\[ToC\]](#) [\[Previous\]](#) [\[Next\]](#)

5. Symbols and quantities used in formulae

A or a

$A(E_j)$ is the instrument effective area (cm^2), i.e. the content of an OGIP format ARF file.
A lowercase $a(E,x,y)$ indicates the [mirror effective area](#)

b (and B_i)

$b(E,B_1,B_2)$ indicates an adimensional correction for [Burst Length](#) dependent effects as a function of

BL thresholds B_i .

C_i

Count rate (cts/s alias cts/s/bin) in PHA or PI channel (or bin) i

dN/dE or $S(E)$

Photon input spectrum in $\text{photon}/\text{cm}^2/\text{s}/\text{keV}$

E_j

E_j indicates the input photon energy (keV) on a discrete grid of j values
 ΔE_j indicates the width of the j -th grid elements.

epsilon

Symbol epsilon indicates an adimensional quantum efficiency

f (and r)

$f(E,r)$ indicates the fraction of [PSF](#) falling within an extraction radius r .

G

$G(E)$ indicates the [Gaussian component](#) of the energy resolution.

P

P_{ij} is the pure redistribution matrix, which is an adimensional probability. This is the content of an OGIP format RMF file.

Q

Q_{ij} is a less customary form of the overall response matrix which has the dimensions of $\text{cm}^2 \text{ keV}$. This is the form in which a response matrix is stored in XAS format.

R

$R(i,E)$ or R_{ij} indicates the overall response matrix (on a continuous or discrete energy scale), which has the dimensions of an area (cm^2). This is the product of the RMF and ARF files.

T

$T(E)$ indicates the [non-Gaussian tail](#) component of the energy resolution.

tau

Symbol tau indicates the adimensional transmission of a component like a [filter](#), [grid](#) or [window](#)

[\[Home\]](#) [\[ToC\]](#) [\[Previous\]](#) [\[Next\]](#)

6. References

1. A reference paper (Boella et al. 1997) on the result of MECS ground calibration has been published on A&A Suppl. 122,327 (ADS access via [1997A&AS..122..327B](#))
2. Results on the in-flight performance of the optics have been presented by Conti et al. 1997 at the SPIE conference 3113, pag. 394 (ADS access not found, [abstract at SPIE](#))

3. A progress report on the MECS background has been presented by Chiappetti et al. 1997 at the BeppoSAX/XTE Lincei conference (Nucl.Phys. B (Proc.Suppl.) 69/1-3 pag. 610 : preprint in [astro-ph/9712251](#))
 4. The ground calibration of the mirror units have been presented by Conti et al. 1994 at the SPIE conference 2279, pag. 101 (ADS access not found, [abstract at SPIE](#))
-

[\[Home\]](#) [\[ToC\]](#) [\[Previous\]](#) [\[Next\]](#)
